Informing groundwater model hydrostratigraphy with airborne time-domain electromagnetic data and borehole logs

Marker, Pernille Aabye

Publication date:
2016

Document Version
Publisher's PDF, also known as Version of record

Informing groundwater model hydrostratigraphy with airborne time-domain electromagnetic data and borehole logs

Pernille Aabye Marker

PhD Thesis
June 2016

DTU Environment
Department of Environmental Engineering

Informing groundwater model hydrostratigraphy with airborne time-domain electromagnetic data and borehole logs

Pernille Aabye Marker

PhD Thesis
June 2016

DTU Environment
Department of Environmental Engineering
Technical University of Denmark

Pernille Aabye Marker

Informing groundwater model hydrostratigraphy with airborne time-domain electromagnetic data and borehole logs

PhD Thesis, June 2016

The synopsis part of this thesis is available as a pdf-file for download from the DTU research database ORBIT: http://www.orbit.dtu.dk

Address: DTU Environment
Department of Environmental Engineering
Technical University of Denmark
Bygningstorvet, building 115
2800 Kgs. Lyngby
Denmark

Phone reception: +45 45251600
Fax: +45 45932850

Homepage: http:// www.env.dtu.dk
E-mail: info@env.dtu.dk

.

Preface

The work presented in this PhD thesis was conducted at the Department of Environmental Engineering at the Technical University of Denmark from 01 October 2012 to 04 May 2016 under the supervision of Associate Professor Peter Bauer-Gottwein and co-supervisor Professor Klaus Mosegaard from the Niels Bohr Institute. The PhD was conducted within the HyGEM research project. The funding for HyGEM is provided by The Danish Council for Strategic Research (project no. 11-116763).

Four scientific papers constitute the PhD work presented herein. The papers are outlined below and will be referred to using the Roman numerals **I-IV** throughout the thesis. Papers **I** and **III** are published in Hydrology and Earth Systems Sciences, Paper **II** is attached as a manuscript and Paper **IV** has been submitted.

I Foged, N., Marker, P. A., Christansen, A. V., Bauer-Gottwein, P., Jørgensen, F., Høyer, A.-S., and Auken, E.: Large-scale 3-D modeling by integration of resistivity models and borehole data through inversion, Hydrol. Earth Syst. Sci., 18, 4349-4362, doi:10.5194/hess-18-4349-2014, 2014.

II Marker, P. A., Ferré, T., Vilhelmsen, T. N., Tuller, M., Bauer-Gottwein, P.: Can groundwater model hydrostratigraphy be determined from electrical conductivity and clay fraction? *Manuscript*.

III Marker, P. A., Foged, N., He, X., Christiansen, A. V., Refsgaard, J. C., Auken, E., and Bauer-Gottwein, P.: Performance evaluation of groundwater model hydrostratigraphy from airborne electromagnetic data and lithological borehole logs, Hydrol. Earth Syst. Sci., 19, 3875-3890, doi:10.5194/hess-19-3875-2015, 2015.

IV Marker, P. A., Villumsen, T. N., Foged, N., Wernberg, T., Auken, E., and Bauer-Gottwein, P.: Probabilistic predictions from groundwater model informed with airborne EM data. *Submitted.*

TEXT FOR WWW-VERSION (without papers)

In this online version of the thesis, Paper **I-IV** are not included but can be obtained from electronic article databases, e.g. via www.orbit.dtu.dk or on request from DTU Environment, Technical University of Denmark, Bygningstorvet, Building 115, 2800 Kgs. Lyngby, Denmark, info@env.dtu.dk.

Acknowledgements

First, I would like to thank my supervisor Peter Bauer-Gottwein; for encouraging me to apply for the PhD position in the first place, and for always be there with an open door to help and discuss. During my graduate studies you gave support and guidance for me to become interested in hydrogeophysics, which without doubt has led me to where I am today. I would also like to thank my co-supervisor Klaus Mosegaard, for always exciting and inspiring discussions, and for getting me hooked on geostatistics and inversion theory during my graduate studies.

The funding for this PhD study by The Danish Council for Strategic Research (Project no. 11-116763) through the HyGEM research project is gratefully acknowledged.

Much of this work has been performed in close collaboration with HyGEM partners from the Department of Geoscience at Aarhus University. I would especially like to thank Nikolaj Foged and Troels Norvin Vilhelmsen, it has truly been a pleasure to work with both of you. I would also like to thank the many others that I have had the pleasure to work with and learn from through the HyGEM project; Anders Vest Christiansen, Esben Auken, Steen Christensen, Thomas Wernberg, Jan Gunnink, Anne-Sophie Høyer, Ingelise Møller, and Flemming Jørgensen. I would also like to thank Xin He and Jens Christian Refsgaard from GEUS for sharing your work and ideas, and for pleasant collaboration.

My external stay, visiting Ty Ferré in Tucson, AZ, at the University of Arizona was a great experience. I am very grateful for all enthusiastic discussions we had and the piles of paper we managed to scribble our way through. Thanks also to Nikolaj Kruse Christensen, for our 4 overlapping weeks in Tucson of discussing ideas, teaching me Python and climbing.

I can only say that I hope to continue working with everyone in the future; there are many things yet to discover, discuss and learn.

The work environment at the Department of Environmental Engineering at DTU is a great place to do a PhD. I would like to thank Poul Løgstrup Bjerg for being a good and considerate leader. Hugo Maxwell, thank you for enthusiastically, patiently and repeatedly explaining me the world of computers. I would also like to thank Anne Harsting for always being helpful and a friendly face.

Claus and Filippo, thank you for being the best office mates and sharing ups and downs along the way. Thank you, all my colleagues at DTU through the years, for the coffee breaks, lunch breaks, 101 trips, and morning swims: Klaus, Anne, Mkhuzo, Kawawa, Manfred, Carson, Bentje, Louise, Nicola, Trine, Vinni, Maria, Carmen, and Lucia.

Finally, my parents, my sister Marianne and Raphael, thank you!

Summary

Hydrological models of groundwater systems and integrated hydrological systems are commonly used tools to manage groundwater resources and support decision making. The models are utilized to quantitatively support management of water supply from well fields; perform dewatering calculations for construction sites; quantify groundwater contamination in time and space; estimate ecological impacts of anthropogenic or climatic stresses; characterize salt-water intrusion phenomena, etc. Applications can be at scales of tens to thousands of square kilometers. The reliability of numerical groundwater models is closely related to the quality and amount of hydrological and geological data available to inform the modeling process. This is particularly true for lithological and geological data required to map the 3-D distribution of aquifer materials, which is also called the hydrostratigraphy. A major challenge for groundwater modelers is that the hydrostratigraphy, which is one of the most critical parameterizations of groundwater models, is based on properties for which direct information is inherently difficult to obtain. The uncertainty resulting from this is non-trivial to estimate and thus rarely quantifiable.

Airborne time-domain electromagnetic (AEM) data obtained using novel methods of data acquisition and processing are attractive because the resulting electrical resistivity models of the subsurface can be obtained at a lateral resolution unmet by geological data while covering areas of hundreds of square kilometers. Application of geophysical data in hydrology however is challenged by the necessary petrophysical translation of the measured physical property into a hydrological property.

The PhD study investigated an approach to incorporate structural information contained in large AEM data sets directly into the groundwater modeling process. The work focuses on reproducibility and objectivity, which is typically lacking in traditional interpretations of AEM and lithological information, and the approaches presented in this thesis are to a large extent automatic. An approach that integrates EM data and borehole lithological information directly into groundwater models is proposed. The approach builds on a clay-fraction inversion which is a spatially variable translation of resistivity values from EM data into clay-fraction values using borehole lithological information. Hydrostratigraphical units are obtained through a *k*-means cluster analysis of the principal components of resistivity and clay-fraction values. Under the assumption that the units have uniform

hydrological properties, the units constitute the hydrostratigraphy for a groundwater model. Only aquifer structures are obtained from geophysical and lithological data, while the estimation of the hydrological properties of the units is inversely derived from the groundwater model and hydrological data.

A synthetic analysis was performed to investigate the principles underlying the clustering approach using three petrophysical relationships between electrical conductivity and hydraulic conductivity. Aquifer structures obtained from clustering on electrical conductivity and clay fraction resulted in mismatch with the true pumping well capture isochrone of 8 to 13 percent. Results for clustering only on electrical conductivity were not stable.

The approach was first tested for the 156 km^2 large integrated hydrological model of the Danish case study Norsminde. The hydrological performance in terms of fit to the transient hydraulic head observations and stream discharge observations results in root mean square errors of 2.0 m and -0.79 m, and mean errors of 0.28 m^3s^{-1} and -0.011 m^3s^{-1} for head and discharge respectively. Benchmarking against comparable Danish models reported in scientific papers confirmed good hydrological performance.

The automatic hydrostratigraphical modeling approach was extended to quantify of the uncertainty of groundwater model predictions. An ensemble of equally likely hydrostratigraphical models was simulated at locations with no data to parameterize the entire model domain, using indicator variograms. The method was applied to the 46 km^2 groundwater model of the Danish site Kasted. Hydrological performance of 75 realizations in terms of fit to steady-state hydraulic head observations and base-flow estimates correspond to root mean square errors around 5.5 m and mean errors of -0.2 m, and percentage errors around 0 to -4 respectively. Differences in local scale connectivity/dis-connectivity of aquifer materials resulted in a probabilistic well catchment area. Results indicate 85% probability that the well catchment area extends beyond the well catchment area determined from a manually developed deterministic geology.

The applications to Norsminde and Kasted sites, combined with the theoretical insight gained from the synthetic analysis, show promising results for direct integration of AEM data into the groundwater modeling process using cluster analysis. Because the presented methods are reproducible and time saving due to being highly automatized, the methods potentially have commercial value.

Dansk sammenfatning

Hydrologiske modeller af grundvands- og integrerede hydrologiske systemer bruges til at forvalte grundvandsressourcer og vejlede relaterede beslutningsprocesser. Modellerne anvendes bl.a. til, at understøtte den kvantitative forvaltning af vandforsyningen fra kildepladser; udføre afvandingsberegninger af byggepladser; kvantificere grundvandsforurening i tid og rum; estimere miljøeffekten af menneske- eller klimapåvirkninger; karakterisere saltvandsindtrængning i kystnære områder, mm. Modellerne opstilles for arealer på ti til flere tusind kvadratkilometer. Pålideligheden af numeriske grundvandsmodeller afhænger af kvaliteten og mængden af hydrologisk og geologisk data til at underbygge modelleringsprocessen. Dette gælder især for litologiske og geologiske data, som bruges til at kortlægge den rumlige fordeling af grundvandsmagasiners geologi – hvilket også kaldes hydrostratigrafien og er en kritisk parameterisering af grundvandsmodeller. Det er en stor udfordring for grundvandsmodellører, at hydrostratigrafien baserer sig på egenskaber, som det er svære at indsamle informationer om. Dette resulterer i modelusikkerhed, der ikke umiddelbart kan estimeres og derfor sjældent kvantificeres.

Tids-domæne luftbårne elektromagnetiske (AEM) data, der indsamles vha. nye dataindsamlings- og databehandlingsmetoder resulterer i modeller af undergrundens elektriske modstand. Disse data er attraktive, fordi de kan produceres i en langt højere lateral opløsning end geologiske data og samtidig afdække arealer på flere hundrede kvadratkilometer. Anvendelsen af geofysiske data i hydrologi udfordres dog af den nødvendige petrofysiske oversættelse af de målte fysiske egenskaber til hydrologiske egenskaber.

Ph.d-studiet undersøgte en metode til at indarbejde strukturel information fra de store AEM datasæt direkte i grundvandsmodelleringsprocessen. Arbejdet fokuserede på reproducerbarhed og objektivitet, hvilket typisk mangler i klassiske fortolkninger af AEM og litologisk information, og metoderne præsenteret i dette studie er i vidt omfang automatiske. Der foreslås en metode der integrerer EM data og litologisk data fra boringer direkte i grundvandingsmodellerne. Metoden bygger på lerfraktionsinversion, som er en rumligt varierende oversættelse af elektriske modstande til lerfraktionsværdier ved hjælp af litologisk boringsinformation. Hydrostratigrafiske enheder findes via en *k*-means clusteranalyse af 'principal components' af modstands- og lerfraktionsværdier. Idet det antages, at enhederne har uniforme hydrologiske egenskaber, udgør enhederne hydrostratigrafien for en grundvandsmodel. Alene grundvandsmagasinets strukturer findes fra geofysiske og litologiske

data, mens estimeringen af enhedernes hydrologiske egenskaber udledes inverst vha. grundvandsmodellen og de hydrologiske data.

Et syntetisk studie blev gennemført for at undersøge den teoretiske baggrund for clustermetoden ved hjælp af tre petrofysiske relationer mellem elektrisk ledningsevne og hydraulisk ledningsevne. Strukturer af grundvandsmagasinet opnået vha. clusteranalyse på elektrisk ledningsevne og lerfraktioner resulterede i 8 til 13 procents fejl ved sammenligning med det sande indvindingsopland. Ved clusteranalyse på elektrisk ledningsevne alene var resultaterne ustabile.

Metoden blev først testet på den 156 km^2 store hydrologiske model for Norsminde området. Den hydrologiske performance, målt ved tilpasning af transiente trykniveau- og vandføringsobservationer resulterede i en kvadratrod af middelkvadratafvigelsen på 2,0 m og 0,79 m, og middelfejl på 0,28 m^3s^{-1} og -0,011 m^3s^{-1} for henholdsvis trykniveauer og vandføringer. Benchmark med sammenlignelige publicerede modeller bekræftede den gode hydrologiske performance.

Den automatiske hydrostratigrafiske modelleringsmetode blev udvidet for at kunne kvantificere usikkerheden ved grundvandsmodellernes prædiktioner. Et sæt af lige sandsynlige hydrostratigrafiske modeller blev vha. indikatorvariogrammer simuleret på lokaliteter uden data for at parameterisere hele modeldomænet. Metoden blev anvendt på den 46 km^2 store grundvandmodel af Kasted. Hydrologisk performance af 75 realisationer målt i forhold til steady-state trykniveausobservationer og baseflow estimater stemte overens med henholdsvis en kvadratrod af middelkvadratafvigelsen på 5,5 m og middelfejl og -0,2 m, og procentfejl på 0 til -4. Forskelle i kobling og afkobling af geologiske materialer der udgør grundvandsmagasinet på en lokal skala resulterede i et probablistisk grundvandsdannende areal. Resultaterne indikerer, at der er 85 pct. sandsynlighed for, at arealet rækker udover det areal, beregnet vha. en manuelt udviklet deterministisk geologisk model.

Anvendelsen af modellen på Norsminde og Kasted kombineret med den teoretiske erfaring fra det syntetiske studie viser lovende resultater for direkte integration af AEM data i grundvandsmodelleringsprocessen vha. clusteranalyse. De præsenterede metoder er reproducerbare og tidsbesparende pga. en høj grad af automatisering, og derfor har metoderne potentielt kommerciel værdi.

Table of contents

Abbreviations

K	Saturated hydraulic conductivity
σ	Bulk electrical conductivity
σ_w	Pore-water electrical conductivity
σ_s	Surface electrical conductivity
ρ	Electrical resistivity
CF	Clay fraction
AEM	Airborne electromagnetic
TEM	Time-domain electromagnetic
CEC	Cation exchange capacity

1 Introduction

Management of groundwater resources is essential for a wide range of human needs and activities.

Groundwater is an important source for domestic, industrial, and agricultural water supply. Worldwide, groundwater abstraction makes up 26% of the total water use (based on 2010 data); of which 70% is used for agriculture, 21% for domestic purposes, and 9% for industry (Margat and van der Gun, 2013, pp123-125). Depletion of groundwater resources is a growing problem especially in India, China, the Middle East and the US South-West (Aeschbach-Hertig and Gleeson, 2012). Prior to installation of new abstraction wells or increasing the production rate of existing wells, it is useful to obtain quantitative information about what negative ecological impacts the changes may have, what abstraction rate corresponds to a sustainable aquifer exploitation, or the best location for installation of the new well.

Clean groundwater resources are essential for many uses of groundwater. Most human activities tend to impact natural systems. These impacts may not always be immediately foreseeable and they may result in contamination of groundwater systems. Contamination of groundwater systems comes in various forms: for example as diffuse sources from agriculture or point sources from pollutant spills. The pollutants travel through the groundwater systems which ultimately determine the state and fate of the pollutants. Before initiating an activity that may cause contamination, we may want to check if the groundwater and/or surface water will be contaminated and to what extent. Or, in order to propose remediation efforts of an existing contamination we may want to check whether a planned remediation initiative will mitigate the existing contamination.

Groundwater however may also be an obstacle. This is the case for construction of buildings and infrastructure, where construction sites require dewatering of sometimes large areas. Here, it is for example necessary to know the required pumping rate to maintain a dewatered construction site within cut-off walls. Given the size of the global construction industry it is easy to see how frequently groundwater models are used.

Groundwater is just one compartment of the hydrological cycle. The compartments of the hydrological cycle are connected making up a complex system of interactions, responses and transport.

In management situations we often need to know where the groundwater is, why it is where it is, how much there is, and of what quality. We may want to answer the question: "If I do this/if this was done in the past (install pump, redirect water body, contaminate this area, infiltrate water here) how can we expect the hydrological system to respond?" In other words, we need to *predict* (in time and/or space) the behavior of the system given an imposed stress. Ultimately it is the space and time distribution of groundwater quantity and/or quality that is of interest to us.

The activities and needs listed above are all examples of situations that utilize distributed numerical models of groundwater and integrated hydrological systems. Distributed models are necessary due to the high spatial heterogeneity of the systems. Using numerical models we can *estimate* an answer to the general question posed above. These models are widely used tools to quantify and predict system response to stresses, and ultimately assist management and decision making.

In these models the distribution of subsurface geological materials plays a large role in whether the prediction made with the numerical models are representative for the true natural system. The distribution of subsurface geological materials that are relevant for hydrological flow is called the hydrostratigraphy.

Because the subsurface cannot be directly observed, hydrostratigraphical mapping presents an ongoing challenge at all scales across hydrological sciences. This is reinforced by the fact that the hydrostratigraphy has a large impact on hydrological flow and transport processes. Groundwater models used for water resources management typically cover from tens to thousands of square kilometers and describe local to regional scale flow systems. Mapping such large aquifer systems requires large datasets about the subsurface.

Scarcity of traditional lithological and geological data, especially with respect to the lateral spatial resolution, is a well-known problem. Thus, geophysical methods have received considerable attention from the hydrological community for the lateral spatial coverage of geophysical data. This type of coverage is unmet by classical hydrogeological data. Initially the hydrological sciences were leaning on mining and petroleum fields for geophysical methods and applications. However attractive, geophysical data is not directly applicable in hydrological contexts because of the unknown relationship between the measured physical property and the hydrological property of interest. Basically, geophysical data does not contain the exact information we

need but is merely a proxy for our desired property. Relationships to translate from proxy to target are often uncertain or even unknown.

Observations of hydrological states – fluxes, concentrations, hydraulic head – and hydrological and geological parameters are essential to understand and conceptualize numerical models of the hydrological systems. Parameterization of distributed hydrological models requires data from many sources, and often involve methods to interpolate/extrapolate to cover the desired area.

1.1 Research objectives

The PhD study has focused on the use of airborne electromagnetic (AEM) data to map the hydrostratigraphy for groundwater models.

The objectives of the research were:

- Development and real-world large scale demonstration of an approach to directly incorporate large AEM data sets into the groundwater modeling process (Paper **I** and Paper **III**)
- Demonstration and test of the approach in a generic synthetic framework (Paper **II**)
- Development and demonstration of an approach to account for hydrostratigraphical uncertainty in hydrological predictions from groundwater models (Paper **IV**)
- Maintaining reproducibility and objectivity in the developed approaches

1.2 Thesis structure

Section 2 'Background' frames the work completed during the PhD with respect to the relevant scientific fields and concepts. It highlights the relevance of the PhD work. Section 3 'Case studies' summarizes the main features of the two Danish case studies Norsminde and Kasted. In section 4 'Methods' an overview of the time-domain electromagnetic (TEM) method is given followed by the relevance of the clay-fraction inversion concept to hydrology. The methods presented in Paper **II**, Paper **III**, and Paper **IV** are subsequently summarized. An overview of the software and CPU time employed to complete the work presented in this thesis is given in section 5 'Software and computations'. The main findings of the PhD work and a brief discussion thereof are presented in section 6 'Summary of main results', followed by conclusions in section 7 and suggestions for future research in section 8.

2 Background

Hydrological models including groundwater compartments are used at laboratory scale, field scale, and regional scale to test hypotheses, understand processes, predict stress scenarios, and, as explained in the introduction, manage water resources. Common for the applications is the need to delineate the hydraulic conductivity (K) distribution in the subsurface. The spatial distribution of K is the backbone for subsurface hydrological models of flow and transport processes. Mapping the subsurface is inherently difficult. Because of this, hydrogeologists are continuously searching for data and methods to map or constrain the subsurface K field.

This thesis deals with saturated hydraulic conductivity, which will simply be referred to as hydraulic conductivity or K. The term 'groundwater model' will be used interchangeable with 'distributed numerical groundwater model' throughout this thesis; the shorter term is used for ease of reading.

Geophysical methods have been applied extensively in hydrogeology to map subsurface hydrological properties and observe and understand hydrological processes. Geophysical data offers subsurface imaging possibilities unmet by lithological borehole information. Information obtained from boreholes inherently has a high vertical resolution, whereas the horizontal resolution is low. Increasing the horizontal resolution requires installation of many boreholes which may be practically and financially infeasible. In a groundwater flow context, modeling the 'correct' spatial continuity/discontinuity of permeable and impermeable aquifer units is essential to the validity of the resulting model predictions.

Geophysical methods were pioneered in the mineral and petroleum industries. The instrumentation was designed to locate for example mineral anomalies with a strong signal. The signal to noise ratio in groundwater studies is generally much lower than in mining applications (Sørensen and Auken, 2004). Much development of instrument accuracy/sensitivity, forward models, and inverse methods has been achieved in the hydrological and geophysical communities.

The field of research for application of geophysical methods and data in hydrology is called hydrogeophysics. The active field of hydrogeophysics is broad, and includes: research from pore-scale to catchment scale; development of inversion algorithms; process understanding; static and transient mapping of unsaturated zone properties; delineation of subsur-

face/aquifer/hydrogeological structures; optimal extraction of information from data and models through coupled/joint inversion of geophysical and hydrological data; establishment of petrophysical relationships at pore- and field scale. It is beyond the scope of this thesis to visit all these topics. Please see Linde et al. (2015) for a review of inverse methods to map geology; Binley et al. (2015) for a broader review of hydrogeophysics; and Rubin and Hubbard (2005) for textbook details.

A common challenge for hydrogeophysical applications (maybe with the exception of time-lapse gravity methods) is how to relate the measured geophysical property to a hydrological property.

2.1 Groundwater models, data, and predictions

Groundwater models do not exist as generally applicable descriptions of the real world. The complexity of hydrological systems and our inability to describe even the parts that are well understood make groundwater models applicable to answer specific questions at best.

Hydrologists rely on observations of state variables (hydraulic head, stream discharge, concentration data, etc.) to falsify groundwater models. We can only make as good models as we have validation dataset. Groundwater models therefore are applicable within the context of available data. Groundwater models are applicable for the question they were set up to solve. Given a certain question like; will the stream discharge (an indicator for ecological prosperity) be negatively influenced if we install a well of a certain abstraction rate at location *xyz*? Or, what is the abstraction rate that will not negatively impact stream discharge? The groundwater modeler constructs a model that accurately describes the processes that are sensitive to or impacts the stresses/compartments of the question. The data used to falsify (and/or calibrate) the model also must be representative given the posed question. The models will not be a description of the entire natural system, but only of the parts of the system of relevance.

Hydraulic conductivity is an effective parameter, which is related to a representative volume of porous media (in the case of groundwater flow), through Darcy's law:

$$Q = AK(\Delta h / \Delta l) \tag{1}$$

Where Q is flow [L^3/T], A is area [L^2], K is hydraulic conductivity [L/T], h is hydraulic head [L] and l is length [L]. In this way, measurements of hydraulic

conductivity from pump or slug tests represent the aquifer volume affected by the pump or slug test. In other words, measured *K* represents an average of all aquifer materials through which groundwater is flowing as a result of the stress imposed by pumping or pushing. This makes it meaningful to determine hydraulic conductivity values inversely in the context of the groundwater model. Observations of hydrological states are used to solve the inverse problem.

Numerical models are conceptually flawed due to inaccuracy in discretization, parameterization data uncertainty, boundary conditions errors, and processes not included in the model. In addition, the observations used to falsify the model are uncertain. This means that we falsify our uncertain models with uncertain data. Depending on the data type this is more or less problematic: The discrepancy between an observation of hydraulic head at a point location (*xyz*) and the true head can potentially be large because it is a point location of a potential field. Stream discharge observations on the other hand are average observations carrying information from a large area upstream. Discharge data however are often obtained by translating stream stages into discharge using a rating curve, which, depending on updating frequency, can be very uncertain. It is well known that inversely estimated *K* values are biased to compensate for these conceptual errors and observation errors.

Once the *K* field has been estimated through inversion (along with other calibration parameters) predictions of hydrological states are calculated. The uncertainty of predictions is increased because predictions are different from the observations used to solve the inverse problem in terms of location in spaces or time and state type, or the calculations involve exerting new stresses on the modeled system.

2.2 Uncertainty in groundwater models

The well-known uncertainties inherent to hydrological models have inspired the development of methods to address the various sources of uncertainty, see for example Beven and Binley (1992, 2014), Keating et al. (2010), and Vrugt et al. (2005). Methods typically address input, parameter and observation data uncertainty, although model structural uncertainty is substantial. For many prediction types the largest source of uncertainty of groundwater models originates from structural errors in the hydrostratigraphy (Refsgaard et al., 2006; Seifert et al., 2012; Zhou et al., 2014). Using 6 hydrostratigraphical models, manually constructed by five different geologists, Seifert et al. (2012) showed that predictions of pumping-well drawdown were markedly

variable across the 6 hydrostratigraphical models. The groundwater model used in the study corresponds to the type typically employed in groundwater management situations. Having five different geologists to each set up an independent geological model however is not common in management situations. Therefore the hydrostratigraphical uncertainty in groundwater models used for management situations typically remains unaddressed.

Geostatistical methods are classical tools in hydrogeology to address hydrostratigraphical uncertainty. Delhomme (1979) and Neuman and Yakowitz (1979) present some of the earliest work of using two-point geostatistics in hydrology. They produced probabilistic estimates of K in the framework of a hydrological inversion, constrained by observations of hydraulic head and K. Popular methods are TProGS (Carle and Fogg, 1996), and sequential Gaussian and indicator simulation (Deutsch and Journel, 1998; Deutsch, 2006; Goovaerts, 1997).

Because variogram based two-point geostatistics cannot always reproduce structures observed in geological and hydrological phenomena (Linde et al., 2015; Western et al., 2001), multiple-point statistics (MPS) methods is receiving considerable attention. MPS can produce geologically realistic realizations of aquifer structures, given that a training image is available, and has been applied successfully in hydrological field cases (Hermans et al., 2015; Huysmans and Dassargues, 2009; Ronayne et al., 2008). Most hydrological field applications of MPS cover areas of below one square kilometer, for example describing systems where a geological profile can be used as training image (Huysmans and Dassargues, 2009). This may be because of the challenge of establishing a training image of an area covering tens or hundreds square kilometers. Dickson et al. (2015) however use airborne magnetic data as training image and chose five geological realizations to address geological heterogeneity for a regional groundwater model. Similarly, He et al. (2015) address the uncertainty of a subdomain of a large scale integrated hydrological model by evaluating 10 realizations of the subsurface, simulated with TProGS using transition probabilities.

2.3 AEM applications in hydrology

Applications of airborne electromagnetic data in hydrology range from delineation of subsurface structure, mapping the extent of groundwater salinity, to description and understanding of complex hydrological systems. To give an idea about how the data has been used, a few examples are given here.

In Northern Europe electromagnetic methods, ground-based and airborne, have played a vital part in mapping the extent, depth, and location of complex buried valley systems (Bosch et al., 2009; Jørgensen and Sandersen, 2006; Sandersen and Jorgensen, 2003; Steinmetz et al., 2014). The valleys make up aquifers, from which water is abstracted intensively for water supply. Glacial meltwater gravel and sand make up a large part of the aquifer material, which often has a high hydraulic conductivity. Intensive abstraction from pumping wells thus can have far reaching effects in the complexly interconnected system of valleys. The interface between the high electrical resistivity aquifer materials incised into fatty clays of low electrical resistivity is determined well with AEM data.

Due to the high electrical conductivity of saline solutions the electromagnetic method has proven suitable to assist hydrological models of salt water intrusion and map salt water intrusion fronts at location where geological heterogeneity can be assumed negligible (Herckenrath et al., 2013; Rasmussen et al., 2013; Sulzbacher et al., 2012). The water resource challenges caused by sea water intrusion in Australia at often very large scales are managed with the help of AEM data, see for example Lawrie et al. (2012) and references therein. The data is commonly used as a mapping tool to delineate the extent and concentration distribution of sea water intrusion.

In the Okavango Delta in Botswana (Meier et al., 2014) and the Machile-Zambezi Basin in Zambia (Chongo et al., 2015) AEM data has contributed to the process understanding of the hydrological system and aided the interpretation of the geological history through mapping of a Paleo-lake salinity anomaly.

AEM data is less often integrated directly into the hydrological modeling process. Joint and coupled hydrogeophysical inversion schemes, as presented in section 2.4, do exist but hesitation is probably because the inversion of an AEM data set in a joint or coupled hydrogeophysical inversion is a computationally heavy task.

2.4 Structural hydrogeophysical inversion

One branch of hydrogeophysical inversion focuses on extracting structural information about hydrological properties from geophysical data. The underlying assumption is that structures identified by geophysical measurements can be characterized by a uniform hydrological parameter. This falls in line with the effective parameterization of numerical hydrological models, when

geophysical data is combined with a subsequent hydrological inversion (Cassiani and Binley, 2005).

Joint hydrogeophysical inversion (see Ferré et al. (2009) for definition) of one or more geophysical data types is commonly employed to solve ambiguities in single data types. Gallardo and Meju (2003) and Doetsch et al. (2010) for example used seismic travel times and electrical resistivity to identify zones of uniform hydrological properties; and Linde et al. (2006) developed a structural inversion using radar velocity and tracer test data to define zones of uniform hydraulic conductivity, which was tested with a synthetic study. Hyndman and Gorelick (1996) estimated the 3-D aquifer zonation along with hydraulic conductivity of the zones from seismic, tracer test and hydraulic data.

Cluster analysis, often fuzzy *c*-means or *k*-means, has also been applied in combination with several geophysical data types to obtain a structural interpretation of geophysical data. Examples are Bedrosian et al. (2007) using magnetotelluric and seismic data and Paasche et al. (2006) using several data sets. The statistical analysis offers a data-driven method to identify subsurface structures.

The identified structures are often not tested with or applied to hydrological simulation. Also the methods are commonly developed for and applied to the field scale.

3 Case studies

The methods presented in this thesis were applied to two Danish case studies; the Norsminde site and the Kasted site. The sites are located on the eastern coast of Jutland, Denmark, see Figure 2 and Figure 4

Quaternary glacial events have shaped the main features of the shallow subsurface of Eastern Denmark. Geologically, Norsminde and Kasted are characterized by a system of buried valleys formed by Quaternary melt water deposits incised into Paleogene fine-grained marls and clays. The valleys make up systems of interconnected aquifers, which are intensely exploited for groundwater abstraction. Valley fills are highly heterogeneous, and the fills include meltwater gravel and sand but also less conductive fine-grained materials (Jørgensen and Sandersen, 2006). Additionally, the Paleogene sediments are overlaid by Miocene sands and clays in the western part of the Norsminde site.

Norsminde as well as Kasted are characterized by a large amount of available hydrological, lithological and geophysical data. Both sites have been associated with research projects; Norsminde with the NICA project (active years are 01 January 2010 to 2014, see http://nitrat.dk/about_us_uk/main.html) and Kasted with the HyGEM project (2011 to 2016).

3.1 Norsminde

The 156 km^2 Norsminde site takes its name from Norsminde Fjord located on the eastern shore of Jylland, Denmark. An aerial foto of Norsminde Fjord looking from West to East is shown in Figure 1. In the center of the site lies the city of Odder, which has 20,000 inhabitants. See Paper **III** for a more detailed description of the Norsminde site.

Annual groundwater abstraction from 66 well amounts to 18,000-26,000 $m^3 year^{-1}$, mainly abstracted from two geological bodies; the 2 km by 14 km Boulstrup valley striking west to east in the southern part of the area and the more surface-near Miocene deposits in the south-western edge of the site. Observation wells in Figure 2 indicate the approximate location of the two bodies. In the flat terrain dominating the eastern part of the site the Paleogene clay is found a few meters below terrain. In terms of land use the Norsminde site is mainly drained agricultural land, built-up area and patches of forested areas.

Figure 1 Norsminde Fjord, looking towards east. Source (Oplandsråd, 2013).

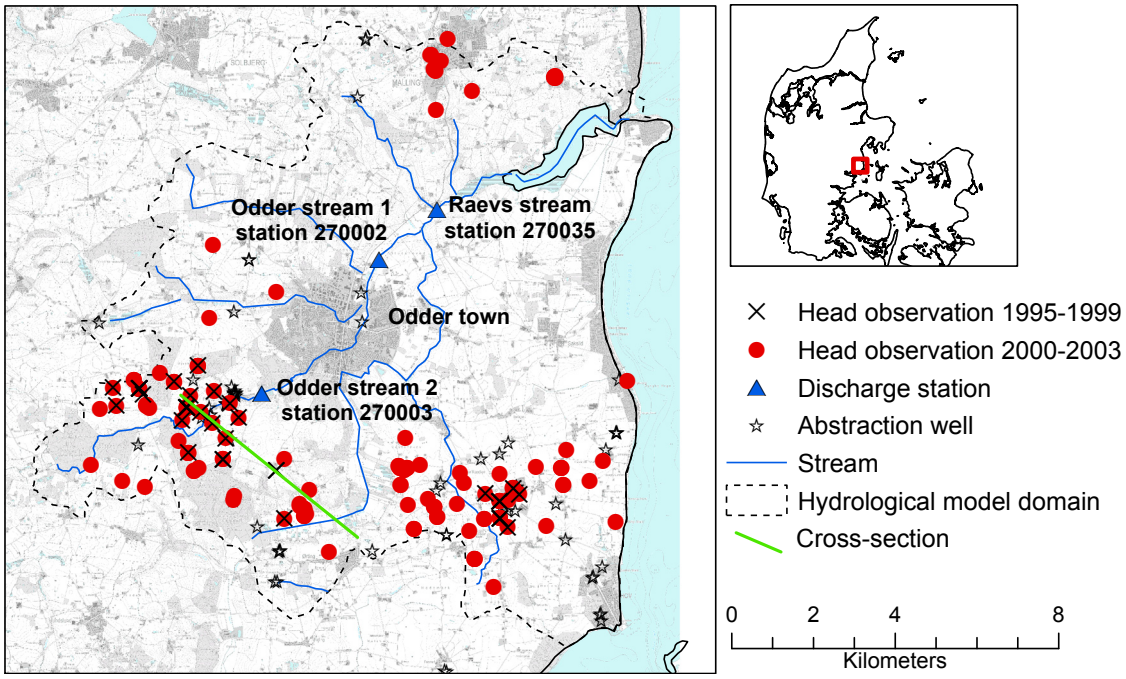

Figure 2 Hydrological base map for Norsminde

3.2 Kasted

As described in Paper **IV** the groundwater model at Kasted consists of a local model embedded in a much larger regional model. The details of the interconnection of the local and the regional models in terms of geophysical data, hydrological data, and groundwater model calibration is described in Paper **IV**. In this synopsis only data from and models of the local area is presented.

The 45 km^2 large local Kasted site is located on the edge of the second largest city in Denmark, Aarhus, with 300,000 inhabitants.

Figure 3 Picture of the landscape at Kasted. Kindly obtained from: Troels Norvin Vilhelmsen, Department of Geosciene, Aarhus University.

The Kasted site is geologically characterized by a system of tunnel valleys of various age, depth, size, and direction. Groundwater is abstracted from the valley aquifers at several well fields, Kasted well field being one of the largest with an annual abstraction of 2-3 million $m^3\ year^{-1}$.

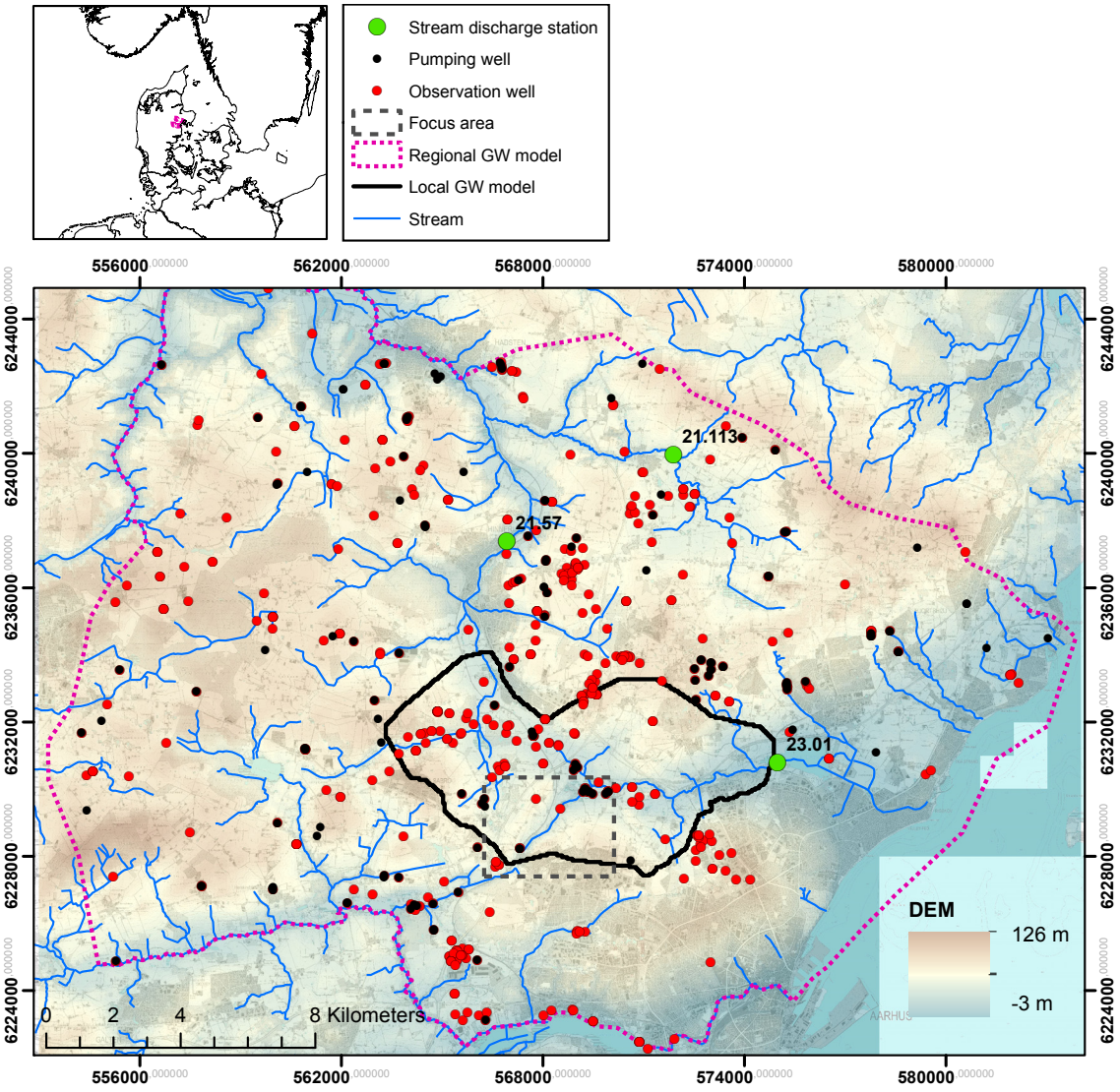

Figure 4 Hydrological base map for Kasted

The data sources presented in Table 1 were used to parameterize the hydrological models of Norsminde and Kasted. The data used to model hydrostratigraphy (geophysical data and lithological information from borehole logs) is not included.

3.3 Data sources

Table 1 Data and data products used for parameterization of the hydrological models for Norsminde (N) and Kasted (K).

Parameterization	Type	Resolution	Source	Acquisition	Open	Site
Topographic map	Grid, spatial	100m	Kortforsyningen	Download	Yes	N, K
Digital elevation model	Grid, spatial	100m	Kortforsyningen	Download	Yes	N, K
Paleogene clay surface	Grid, spatial	100m	GEUS	Contact/subscription	No	N
Precipitation	Grid, spatial/temporal	10km/daily	DMI	Contact	No	N
Global radiation	Grid, spatial/temporal	20km/daily	DMI	Contact	No	N
Air temperature	Grid, spatial/temporal	20km/daily	DMI	Contact	No	N
Vegetation LAI and root depth	Grid; spatial/temporal	500m/seasonal	DK-model (GEUS)	Contact	No	N
Soil type	Grid; spatial	500m	DK-model (GEUS)	Contact	No	N
River network	Vector, spatial		Orbicon, homepage	Download	Yes	N, K
Lithological boreholes	Point data; spatial	Varying	GEUS/Jupiter	Download/database	Yes	N, K
Geophysical soundings	Point data; spatial	Varying	GEUS/Gerda	Download	Yes	N, K

Table 2 Hydrological observation and forcing data used for calibration.

Observation	Type	Resolution	Source	Acquisition	Open	Site
Stream discharge	Point data, temporal	Daily	Naturstyrelsen (Regions)	Contact	No	N,K
Hydraulic head	Point data, temporal	Varying	GEUS/Jupiter	Download/database	Yes	N,K
Groundwater abstraction	Point data, temporal	Yearly	GEUS/water works	Download/contact	Yes/no	N,K
Outlets from wastewater treatment plants	Point data, temporal		Odder spildevand	Personal contact	No	N

4 Methods

The connection and overlap between Paper **I**, Paper **III**, and Paper **IV** is shown with the flow chart in Figure 5. Paper **I**, red box, presents the 3-D formulation of the clay-fraction inversion and proposes the use of cluster models as groundwater model hydrostratigraphy. Paper **III**, blue box, explains the details of the clustering on electrical resistivity (ρ) values and clay-fraction values to obtain hydrostratigraphical units and presents the direct integration into hydrological models and inversion by assuming uniform K of the units. Paper **IV**, green box, extends and modifies the approach in order to be able to stochastically address prediction uncertainty originating from structural groundwater model uncertainty. As the flow chart shows, Paper **I**, Paper **III**, and Paper **IV** all benefit from a similar flow of data and methods. Paper **II** also follows the workflow of clustering on clay-fraction values and electrical conductivity (σ) values to obtain hydrostratigraphical units with uniform groundwater model K values, although for a synthetic case, which makes the input data and groundwater model different from the other papers. The procedure employed to create a synthetic truth is summarized in section 4.4 'Evaluating clustering approach synthetically', but readers are referred to Paper **II** for a thorough description.

Electrical resistivity (ρ) is commonly used in context of the time-domain electromagnetic (TEM) method, whereas electrical conductivity (σ) is commonly used in studies dealing with petrophysical pore- and laboratory scale research. The two properties are unambiguously related: $\sigma = 1/\rho$. Because this thesis deals with TEM data as well as petrophysical relationships at the soil-sample scale, both properties will be used without further explanation.

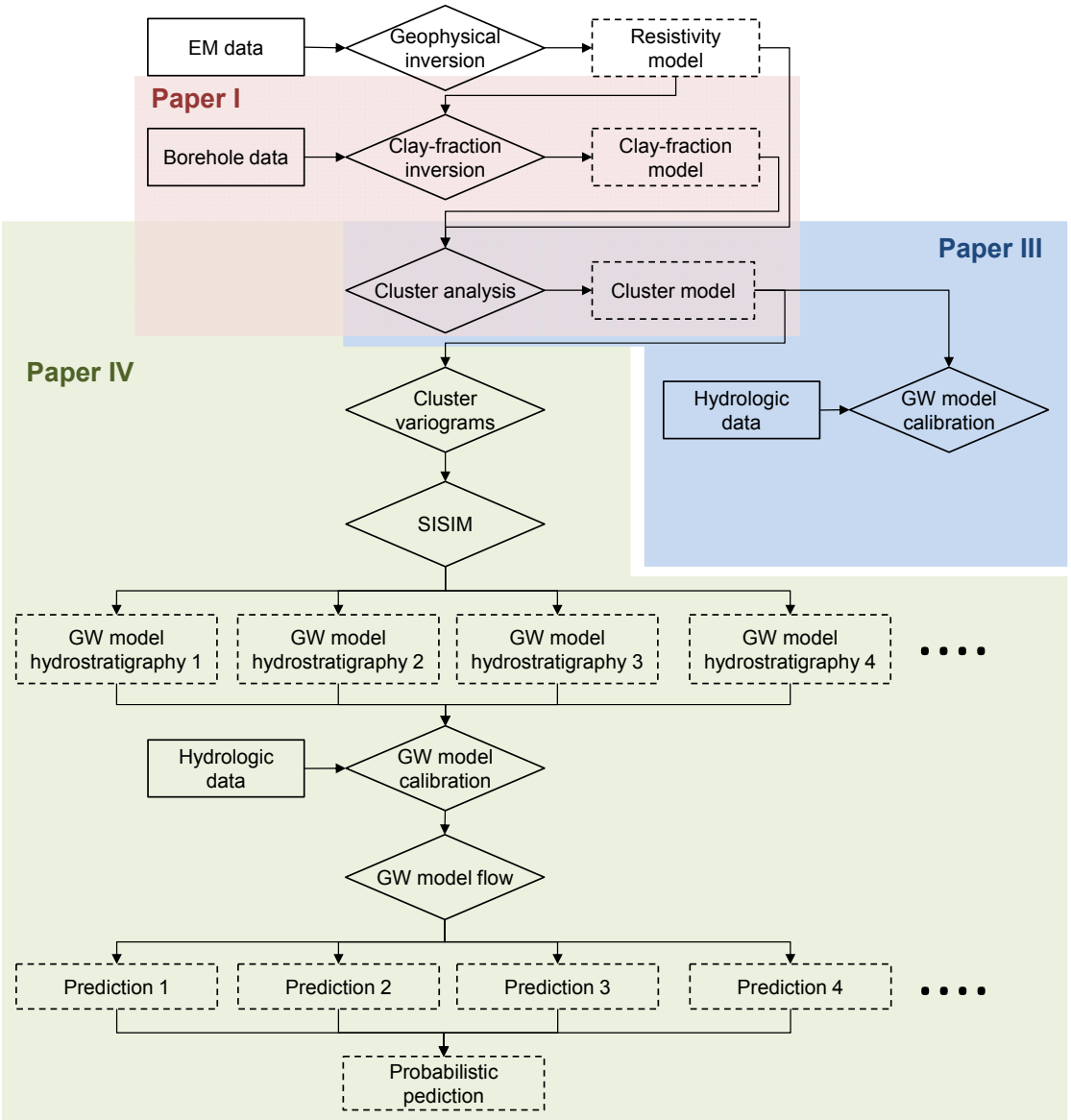

Figure 5 Flow chart illustrating how the methods presented in Paper **I**, Paper **III**, and Paper **IV** are connected.

4.1 TEM data and interpretation

The TEM method is an induction method applied using ground-based and airborne systems. Aside from more advanced instrumentation and data analysis ground-based and airborne systems produce the same data, and a general presentation of the TEM method is given here. The presentation focuses on basic aspects and interpretation, which is relevant for understanding the work presented in this thesis. For a more complete picture the transient electromagnetic method is thoroughly described in the book chapters Christiansen et al. (2006) and Meju and Everett (2005).

The TEM method relies on the capability of subsurface materials (solid and liquid combined) to transmit electrical currents. The method operates at relatively low frequency (10^2 to 10^6 Hz) (~1 µs to 10 ms), which makes the distribution of currents in the subsurface dominantly diffusive. This is because the dielectric permittivity (storage property) is orders of magnitudes smaller at low frequencies (Meju and Everett, 2005).

The measured signal (stacked soundings shown with red error bars in Figure 7 shown as apparent resistivity) is the decaying strength of a magnetic field measured over time, which is the result of an on/off current transmitted in a loop. Figure 6 shows the concepts of how TEM data is collected using an airborne system. The transmitted current results in a primary magnetic field (red dashed lines), which induces current in the subsurface materials (grey arrows in subsurface). These pulsing currents diffuse into the subsurface resulting in a secondary magnetic field (blue dashed lines); and it is the decaying strength of this magnetic field that is measured over time.

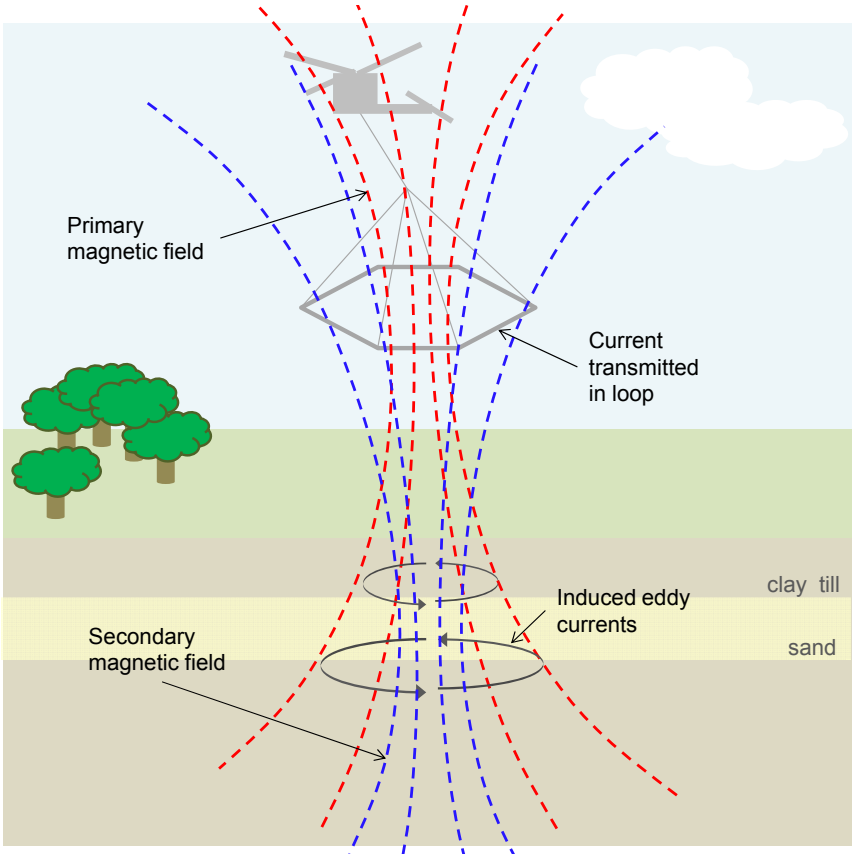

Figure 6 Conceptual drawing of airborne EM data acquisition (The figure is a remake of a figure in DWF (2013))

The strength in volts of the secondary magnetic field is measured. The process of repeatedly (1,000-10,000 times) turning the current on and off and recording of the magnetic field strength at time gates (this is one transient) is called a sounding (Christiansen et al., 2006). The transmitter current strength ranges from 1 A to ~120 A across ground-based and airborne systems; the stronger the current, the higher the resulting magnetic moment, and the larger the penetration depth. The penetration depth is also a function of the subsurface materials and their ability to conduct electrical currents. The vertical resolution diminishes with depth. Two soundings are usually made at each measurement location; a high moment and a low moment. This allows for shallow resolution while obtaining a strong signal at late time gates (at large depths), which is necessary due to noise. The TEM method is unique in terms of depth of investigation, which, depending on the geological setting, can be up to 200-300 meters.

Background noise and coupling responses are important parts of the TEM method. Background noise refers to electromagnetic fields from external sources that influence a measurement. Random noise is averaged out through stacking of transients. Coupling refers to electromagnetic fields generated by the transmitted current but caused not by subsurface materials; examples are buried metal pipes, fences, cars, and power lines. The deterministic coupling responses cannot be averaged out by stacking. Soundings corrupted by couplings must be removed before inverting the data. This can be seen in the processed datasets where for example power lines stand out as data-free bands through the otherwise dense datasets.

The result of interpreting and inverting TEM soundings is a model of the subsurface electrical resistivity as a function of depth (1-D). Figure 7b shows an example of a many-layer 1-D resistivity model showing an intermediate resistivity layer at the surface followed by a thin layer of low resistivity material, and a thick layer of high resistivity overlaying low resistivity material. The information carried in the measured signal is related to the corresponding current distribution of the subsurface. In a subsurface of layers with different resistivity the current density is highest in low resistive materials, while currents diffuse fast through materials of high resistivity. This means that the corresponding secondary field is largely shaped by low resistivity materials, or we can say that the measured signal is more sensitive to low resistivity materials. Take for example the model shown in Figure 7b: the estimated 100 Ωm of the thick high resistivity layer located at 40-75 meters below terrain is

more uncertain than the estimated 10 Ωm of the thin layer above. The sensitivity is also a function of depth and time (because the density decreases as the currents diffuse into the material over time).

This inevitably has impacts for application in hydrology. Due to variable resolution with depth we must expect that the same material may appear to have different resistivity values depending on whether it is surface near or located at greater depths. Another known feature of resistivity models is the shielding effect. This refers to the decreased sensitivity of a high resistivity material underlying a low resistivity material. The currents will be focused in the low resistivity layer and therefore little information is available of the underlying high resistive material.

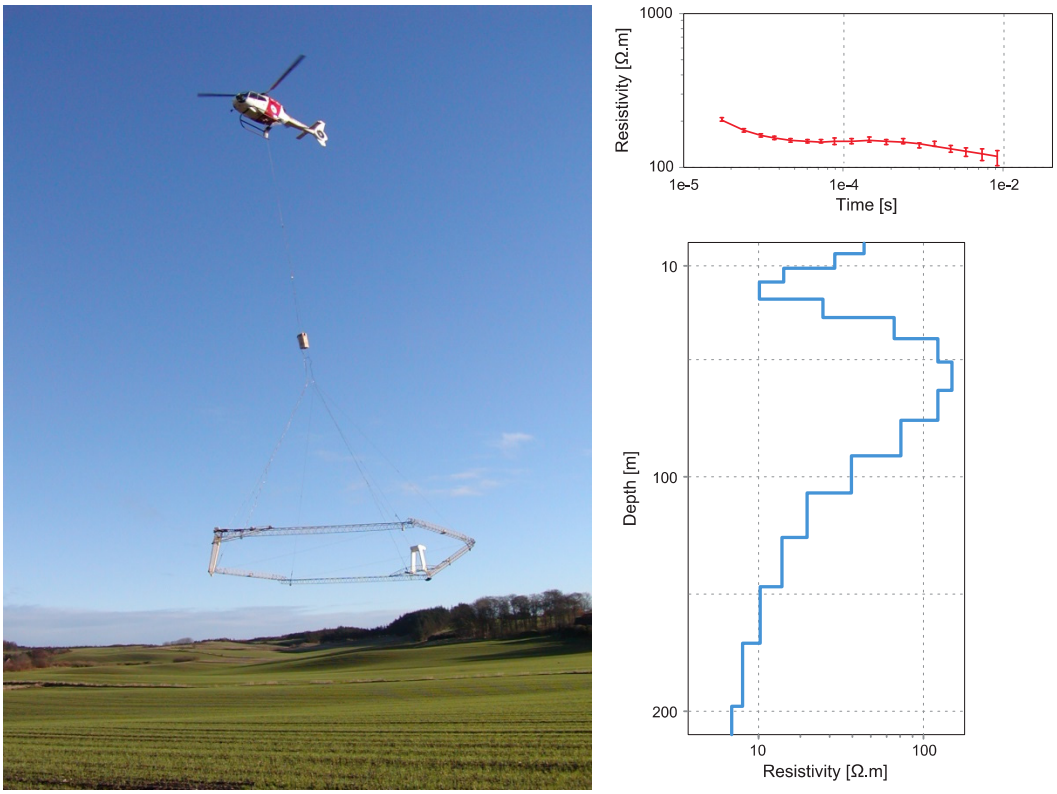

Figure 7 Left: The airborne system, SkyTEM, in flight. Right: Example of EM sounding (red error bars), forward model (red line), and 1-D resistivity model (blue line) (Auken et al., 2009).

To obtain a resistivity model as a function of depth TEM data must be inverted. The data is typically interpreted through 1-D forward models, which is reasonable for exploration of stratified subsurface materials. As is the case

for other geophysical data types, the inverse problem is underdetermined, and the solution to the 1-D problem therefore is nonunique. In case of the large airborne data sets where up to hundred thousand soundings are collected for one site, regularization is introduced to solve the non-uniqueness by simultaneous inversion of soundings. Spatial constraints between model parameters are introduced to mimic geological structures. Examples are quasi 2-D (Auken and Christiansen, 2004) and quasi 3-D (Viezzoli et al., 2009) formulations where lateral continuity in the resistivity between neighboring models is rewarded as wells as sharp transition in vertical resistivity values.

4.2 Clay-fraction inversion

Geophysically derived resistivity maps of the subsurface are used in hydrogeology to identify salinization, lithology, and are sometimes related to hydraulic conductivity. The diffusion of electrical currents through porous materials is controlled by the conductive properties of the porous material and the liquid with which it is filled.

Archie's empirical equation for the electrical conductivity of saturated porous materials (Archie, 1942) relates electrical conductivity to geometrical properties of a porous material; $\sigma = \sigma_w \phi^m$ where σ_w is the pore-water electrical conductivity, and the formation factor is defined as $F = \phi^{-m}$ from the cementation index m and porosity ϕ. The relationship is applicable for porous media saturated with strong electrolytes. Including the contribution from surface conductivity, σ_s, and under the assumption that σ_w and σ_s act in parallel, i.e. there is no inter-dependency between σ_w and σ_s, Waxman and Smits (1968) presented the following model:

$$\sigma = \phi^m \left(\sigma_w + BQ_v \right) \tag{2}$$

where B was estimated empirically as $B = \left(1 - 0.6 \cdot \exp\left(-\sigma_w / 0.013\right)\right) \cdot 0.046$ and defined as 'equivalent conductance of clay exchange cations'. The empirical formulation is based on fit to data for soils with high cation exchange capacity (CEC) with low electrolyte concentrations. Q_v, 'the volume concentration of clay exchange cations', was estimated from CEC as $Q_v = \rho_g \left((1-\phi)/\phi \right) \cdot CEC$, where ρ_g is grain density. Other mixture models for electrical conductivity estimate the surface conductance empirically from the clay content, for example Doussan and Ruy (2009) and Rhoades et al. (1976, 1989). However it is not the mineralogy of clays that result in a higher

surface conductance but simply the fact that the surface area of clays is larger than that of for example silicate minerals (Glover, 2015). Because of this, the clay content is used as an approximation of CEC/surface area. The CEC of clay mineral varies up to one to two orders of magnitude from low CEC clays like Kaolinite ranging between 0.03 $mol \cdot kg^{-1}$ and 0.1 $mol \cdot kg^{-1}$ (Ma and Eggleton, 1999), over Illite ranging between 0.10 $mol \cdot kg^{-1}$ and 0.25 $mol \cdot kg^{-1}$, (Kahr and Madsen, 1995) to high CEC clays like Montmorillonite 66 meq $100g^{-1}$ to 123 meq $100g^{-1}$ (Borden, 2001) and Bentonite. It does however seem reasonable to assume some degree of similarity in the clay minerals represented within a field site, for which the same depositional/sedimentary history exists. Paper **II** deals with the CEC and clay content relationship in relation to hydrological applications.

Generally we can say that hydraulic conductivity is a function of pore-space geometry while electrical conductivity is a function of pore-space geometry and chemistry.

It is not possible to uniquely distinguish lithological materials from resistivity data. This can for example be been from the data presented in Hermans et al. (2015) for an alluvial aquifer in Belgium: comparing $\log_{10}$ electrical resistivity data (obtained from DC measurements) with lithological information at the location of boreholes shows overlap in the frequency histograms of sand, gravel, and loam/clay, see Figure 8a. Using data from sites in Denmark Møller et al. (2015) compiled electrical resistivity measurements, from laboratory and borehole DC electrical methods, of clay tills. The borehole resistivity measurements of clay tills from multiple depths at several Danish sites are shown in Figure 8b, which show a narrow distribution indicating that clay tills may be well determined from borehole resistivity logs.

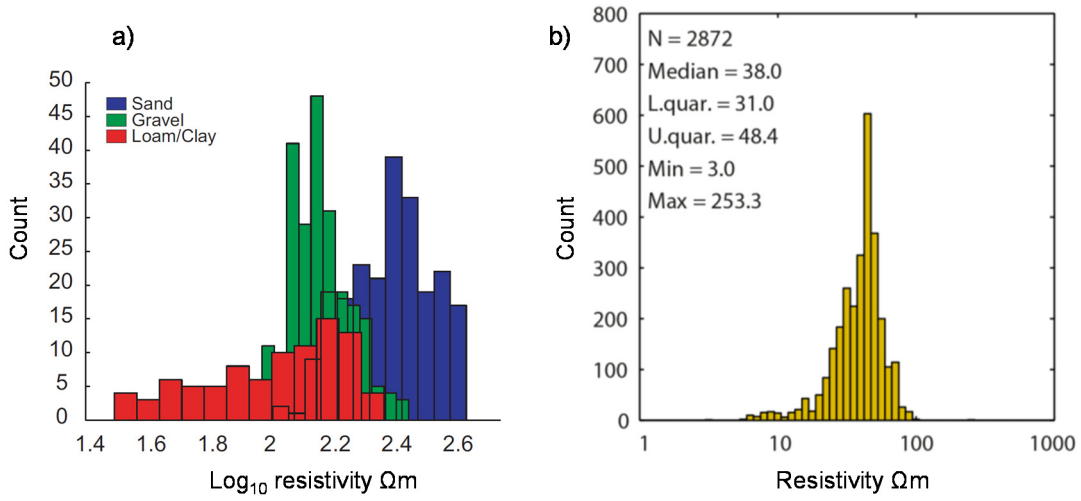

Figure 8 a) sand, gravel and loam/clay distributions for the field sites studies in Hermans et al. (2015), and b) distribution for clay tills from Møller et al. (2015).

In the work presented by Beamish (2013) and Barfod et al. (2016, in review) electrical resistivity data from AEM surveys (frequency and transient methods respectively), histograms of measured resistivity of geological units and lithological types respectively were compiled. In Beamish (2013) the resistivity data is compared to surface geological maps of Northern Ireland, and the results for sandstone (red) and mudstone (blue) are shown in Figure 9a. The overlapping histograms of clay tills (blue) and meltwater sand and gravel (red) shown in Figure 9b are from Barfod et al. (2016, in review). The data for Figure 9b are weighted with respect to borehole quality, resistivity value uncertainty, borehole clustering, TEM resolution, and interpolation error. The unweighted histogram, which is shown in Barfod et al. (2016, in review), shows an overlap similar to the one shown in Figure 9a. Barfod et al. (2016, in review) compared data for entire Denmark and found that the width and overlap of the clay till and meltwater sand and gravel distributions vary greatly between sites across Denmark.

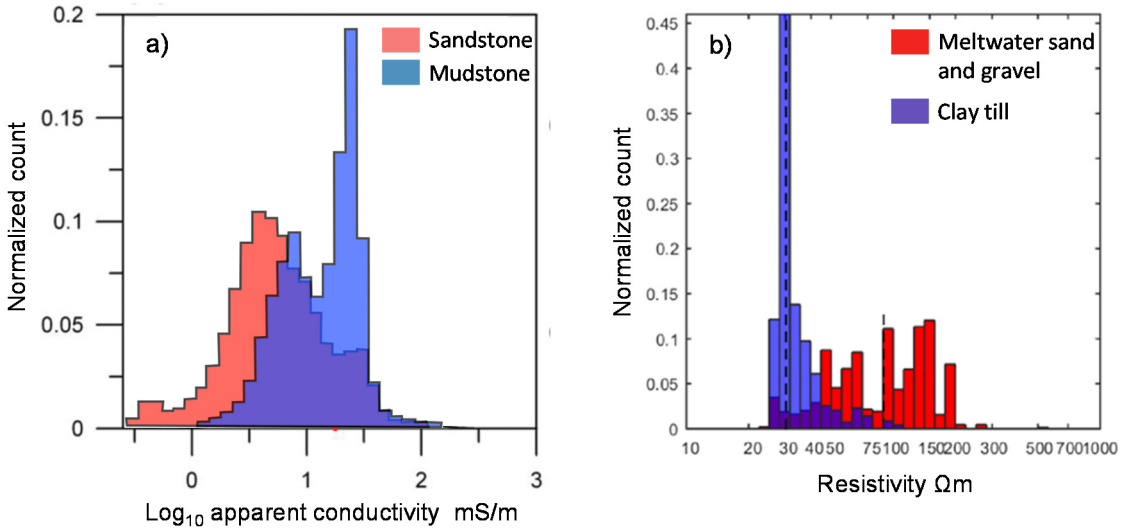

Figure 9 a) modified from Beamish (2013) showing histograms of mudstone (blue) and sandstone (red). b) figure from Barfod et al. (2016, in review) showing histograms of clay tills (blue) and meltwater sand and gravel (red).

The electrical conductivity of a porous material cannot be attributed to the influence of *only* lithology *or* pore-water conductivity, although this is often desired in applications (for example salinity or lithology). The sampled histograms presented in the papers mentioned above and shown in Figure 8 and Figure 9 be influenced by pore-water conductivity contribution to the bulk electrical conductivity of the materials. Also, the variation in the width of the lithological histograms found by Barfod et al. (2016, in review) between sites may also be an indication of variable pore-water influence.

Recognizing the nonunique mapping of lithological groups and the variation in the relationship between field sites, Christiansen et al. (2014) presented an inversion approach to estimate a spatially variable translation of geophysical resistivity values into lithological material using borehole logs as observations. The intended application of the 2-D formulation made by Christiansen et al. (2014) was to estimate aquifer vulnerability towards nitrate contamination. In Paper **I** a 3-D formulation was adapted, with the aim of using the 3-D clay-fraction map to inform groundwater model hydrostratigraphy.

The lithological material is clay fraction (the equivalent, accumulated clay thickness, was used by Christiansen et al. (2014)). Clay fraction is defined as the amount of clay material (i.e. not clay mineral) present over a defined depth interval. The interval length approximately follows the vertical resolution of the geophysical resistivity data. A clay-fraction value carries no information about the vertical distribution of the clay material within the de-

fined depth interval. Figure 10a (from Paper I) shows observed clay-fraction values $\Psi_{\log}$ for five depth intervals. The figure also illustrates that the lithological information in borehole logs must be categorized in terms of clay-fraction values; as exemplified in Figure 10a "clay till" and "clay" is categorized as "clay". Sand and gravel are interpreted as a clay-fraction value of 0.

The quality of the borehole information is used to calculate data weights in the inverse problem. The quality of a borehole is defined from the following information:

- Elevation and geographical location accuracy
- Drilling method
- Borehole purpose (e.g. scientific or water abstraction)
- Reliability of drilling contractor

The two-parameter translation of electrical resistivity (ρ) with parameters m_{up} and m_{low}, is shown in Figure 10c. The translator function is defined on a regular grid, which allows for m_{up} and m_{low} to vary spatially. The translator function is described by a scaled complementary error function:

$$W(\rho) = 0.5 \cdot \mathrm{erfc}\left(\frac{K \cdot \left(2\rho - m_{up} - m_{low}\right)}{\left(m_{up} - m_{low}\right)} \right) \tag{3}$$

where $K = \mathrm{erfc}^{-1}(0.0025 \cdot 2)$. The translator function is applied to each resistivity model layers within a calculation interval. The simulated clay fraction for an interval thus becomes:

$$\mathrm{CF_{res}} = \frac{1}{\sum t_i} \cdot \sum_{i=1}^{N} W(\rho_i) \cdot t_i \tag{4}$$

Where N is the number of resistivity model layers in a calculation interval, and t is the thickness of the resistivity model layer. The objective function used for the inversion is presented in Paper **I**. The objective function is made up of a data misfit term and a regularization term. The regularization terms includes vertical and horizontal constraints. The data misfit term is determined from clay-fraction values observed in borehole logs ($\Psi_{\log}$ in Figure 10a) and the simulated clay-fraction values $\mathrm{CF_{res}}$ (Ψ_{res} in Figure 10a) obtained by applying the translator function to the resistivity values. The misfit

is evaluated at the borehole location. The full procedure is described in Paper **I**, and is briefly outlined here:

1. A value for m_{up} and m_{low} is proposed at each *node location* in the regular 3-D grid (Figure 10b).
2. m_{up} and m_{low} are interpolated (bilinear) to each *resistivity model location*.
3. At the *resistivity model location*, the resistivity value is translated to obtain a simulated clay-fraction value.
4. A simulated clay-fraction at each *borehole location* must be determined. Each *resistivity model location* is associated with a borehole based on a user-defined search radius. A variogram model is fitted to the associated simulated clay-fraction values and a simulated clay-fraction value at the *borehole location* is predicted using point kriging.
5. The misfit between and observed and simulated clay-fraction is calculated at the *borehole location*, which combined with the regularization term makes up the objective function.
6. The process continues iteratively from step 1, until the objective function is at a minimum.

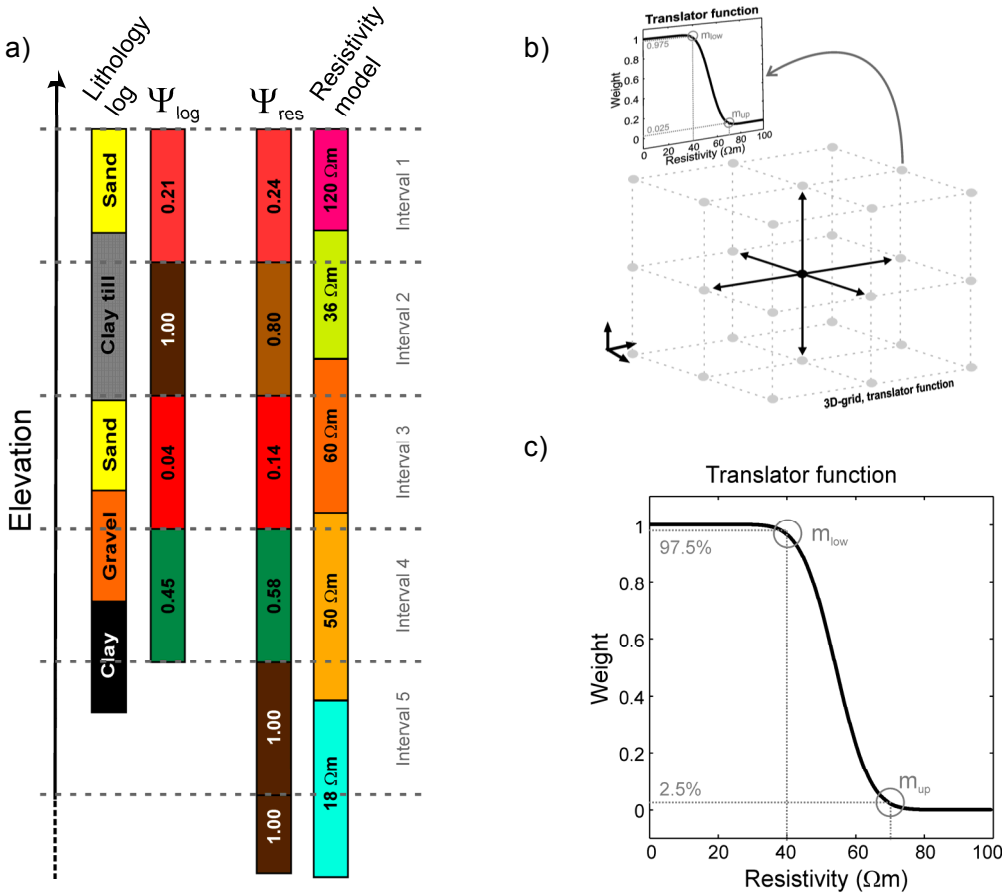

Figure 10 The clay-fraction concept. a) illustrates calculation intervals and how observed clay fraction is compared to simulated clay fraction, b) the calculation grid of the clay-fraction inversion, and c) the translator function. The figures are from Paper **I**.

The influence of pore-water conductivity is corrected for by allowing a spatially variable translation of resistivity values and by using borehole lithology as observations in the inverse problem. If the contribution of pore-water conductivity in an area of the domain influences the resistivity values; the resistivity values are low due to high salinity or electrolytes in the pore-water. The material itself may not be very conductive; it may for example be sand which has a high resistivity. We want these resistivity values to be translated to a simulated clay-fraction value of 0. If clay-fraction observations from borehole logs are present m_{up} and m_{low} will be shifted towards low values (to minimize the objective function) and translate a low resistivity to a clay-fraction of 0, see Figure 10c. If the pore-water electrical conductivity does not majorly contribute to the bulk resistivity m_{up} and m_{low} will be shifted towards intermediate or higher values in order to translate a low resistivity into a clay-fraction value of 1.

4.3 K structure from resistivity and clay fraction

As described in section 2.1, measurements of effective hydraulic conductivity parameters for groundwater models are inherently problematic. Hydraulic conductivity values are commonly estimated through inversion using observations of hydrological states in context of the groundwater model.

Deterministic hydrostratigraphical models represent the regularizing zonation in groundwater models. All deterministic models are uncertain as maps of subsurface structures are inherently flawed. Manually generated hydrostratigraphical models have the advantage of integrating all available data/information irrespective of differences in scale and resolution, lithological borehole information, multiple geophysical data, geological knowledge, etc. A disadvantage is that two geologists are unlikely to construct the same model. So which one is more right? What are the uncertainties associated with each model? Also, groundwater flow is a 3-D phenomenon, and predominantly sensitive to the 3-D connectivity (more than the K value of each zone). Manual hydrostratigraphical models have the 3-D structural information in the AEM resistivity models to guide the interpretation, but capturing all connecting/disconnecting aquifer/aquitard materials of various sizes/scales is a very complex and time-consuming task.

The large AEM data sets can cover the majority of groundwater model domains (study sites in Paper **III** and Paper **IV** are 45 km^2 and 156 km^2 respectively). This opens op for data-driven methods where manual interpretation (or information about continuity of geological features through training images used in MPS methods) of large data gaps are less crucial.

Clustering techniques from pattern recognition are used to find groups in (often multivariate) data. Many text books on statistical data analysis cover cluster analysis, see for example Hartigan (1975) and Duda et al. (2001). In contrast to classification techniques, clustering is unsupervised, meaning that the data is un-labeled and there is no labeled data used for training (Jain, 2010). The data thus drives the analysis. Clustering is routinely applied in remote sensing; to take an example from a field closely related to applied geophysics. One example is the analysis of multispectral images. Delineating land surface features of geomorphology, vegetation type or land-use types can be accomplished by clustering on images taken with different wavelengths. Depending on the wavelengths and the combination of wavelengths different land surface features can be distinguished. It is thus key to identify one or more measureable entities for which the data in multi-dimensional space will

fall into groups that correspond to groups in the target property/phenomenon. In other words, we want the cluster variables to be discriminatory for the target property/phenomenon.

The hypothesis underlying the clustering approach presented in this PhD is that zones identified by clustering on resistivity and clay-fraction values correspond to zones in hydraulic conductivity for which uniform hydraulic conductivity values can be determined in a hydrological model calibration.

Hydraulic conductivity is a function of the pore-space geometry and connectivity. The same is correct for electrical conductivity, which in addition is a function of the geochemistry of the liquid and porous media. The dependency of K and σ on the pore-space geometry and connectivity is related, although how exactly is unknown. We do not expect to be able to discriminate K from σ alone. Clay fraction solves some ambiguity in the σ signal. The clay content of the porous material affects K and σ differently; σ is related to clay content geometrically as well as chemically, while K is related to clay content geometrically.

In this work the k-means algorithm is used to perform the cluster analysis. Similarity in the cluster variables are found by minimizing the within-cluster variance. This results in using squared Euclidean distance as a similarity measure:

$$\min_{\{m_k\},1\le k\le K} \sum_{k=1}^{K} \sum_{x\in C_k} \sqrt{\sum_{i=1}^{p} (x_i - m_{k,i})^2} \tag{5}$$

where $k = 1,\ldots,K$ is a cluster with corresponding cluster center m_k, $x = x_1,\ldots,x_n$ are the data for each of the cluster variables $i = 1,\ldots,p$. The iterative steps of the k-means algorithm are:

1. Determine k random clusters centers $m_1,\ldots, m_k$ (this is called seeding)
2. Calculate distance between $x_1,\ldots, x_n$ and $m_1,\ldots, m_k$
3. Data points are assigned to be a member of a cluster based on shortest distance to cluster centers
4. Update cluster centers; calculated as the mean of the new x members

The process is iterated from step 2 to step 4 until there are no data points that change cluster memberships.

The MATLAB implementation of k-means "*kmeans*" was used to perform the analysis. The solution to the *k*-means problem is known to be dependent on the selection of the first cluster centers. The MATLAB R2014b implementation includes a careful seeding approach (Arthur and Vassilvitskii, 2007). Despite of this, the cluster problems where the number of clusters was larger than approximately 4 resulted in different cluster models for different seedings. The different cluster models varied with respect to the similarity measure to be minimized, i.e. the objective function of a cluster analysis. Because differences in the objective function were small, the hydrological performance of the cluster models with varying objective functions was computed. This was done just for the Norsminde site. Except for the 8-cluster case, the cluster models with the lowest objective function also resulted in the best hydrological performance. The hydrological performance of cluster models with the same number of clusters but with slightly different objective function was not computed for the Kasted site. The differences however were inspected visually. For the 7-cluster case and 8-cluster case, cluster models with objective function differences of approximately 5% resulted in a clearly different subdivision of the clustered space; the region represented by low clay fraction and high resistivity was subdivided into two instead of one cluster. This was not further investigated. The cluster analysis for each cluster model was run with 100 replicates to ensure a stable solution, and to always results in the solution with the lowest objective function.

Because the resistivity data and clay-fraction values are inherently correlated, the clustering is performed on the principal components of normalized resistivity data and clay-fraction values, see Paper **II**.

Figure 11 illustrates a conceptual example of the bivariate information contained in resistivity data and clay-fraction values. The figure shows how the mutual information discriminates between lithologies and pore-water effects in order to define groups that can be assigned uniform K values. Region a) and region c) might end up with similar K values, and ultimately represent one K group, although this is not a drawback for the method.

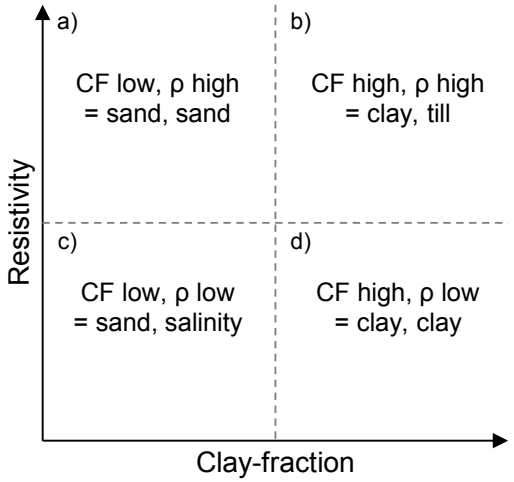

Figure 11 Illustration showing a conceptual example of the two-variable clustering using resistivity and clay-fraction

The approach of clustering on resistivity data and clay-content values is presented through three examples in this thesis: 1) a synthetic case (Paper **II**), 2) the Norsminde case (Paper **III**), and 3) the Kasted case (Paper **IV**). There are a few technical differences between how the approach was applied in Paper **III** and Paper **IV**: in Paper **III** the cluster analysis is performed on a regular grid. Preceding the cluster analysis, resistivity and clay-fraction values were kriged onto a regular grid. In Paper **IV** the cluster analysis is performed at regular elevation intervals at geophysical sounding sites (i.e. regular in z, scattered in x and y). The clusters were subsequently simulated onto a regular grid using indicator variograms models for each cluster; and the deterministic model was identified as the mode of the ensemble of probabilistic simulations.

As shown by the blue box in Figure 5 (Paper **III**) the cluster models are directly used to represent the hydrostratigraphy of hydrological models. A cluster is assumed to have uniform hydrological properties. The hydraulic conductivity of each cluster, or zone, is estimated in the hydrological inversion using hydrological data.

4.4 Evaluating clustering approach synthetically

With a synthetic analysis it is possible to evaluate how well the cluster models perform in terms of capturing the true hydrological model predictions. As mentioned earlier, the relationship between electrical conductivity and hydraulic conductivity at a given field site is unknown and uncertain, and the relationship between electrical conductivity and hydraulic conductivity is

known to vary between sites. In the synthetic analysis three potential petrophysical relationships were established using three models for electrical conductivity, as an attempt to capture some of the known variability in the petrophysical relationship. The analysis defines two characteristics of the petrophysical relationship; nonlinearity and nonuniqueness, which can influence the applicability of the clustering approach in hydrology. In terms of discriminatory power in the cluster analysis these two characteristics result in misclassification related to *differential resolution* and *overlap*, respectively. In the event of a nonlinear relationship between K and σ clustering on σ will produce clusters with uniform spacing in σ while the corresponding clusters will have a non-uniform spacing in K. Depending on the shape of the nonlinear relationship the clusters will have a coarse resolution of high K values and a fine resolution of low K values, or vice versa. In the event of a nonunique relationship between K and σ, the clusters obtained from clustering on σ cannot uniquely discriminate between K values. I.e. the same K values can end up in different clusters, because clusters overlap in K-space. The analysis in Paper **II** addresses how resolution and overlapping in the clustering approach impact hydrology. See Paper **II** for elaborations.

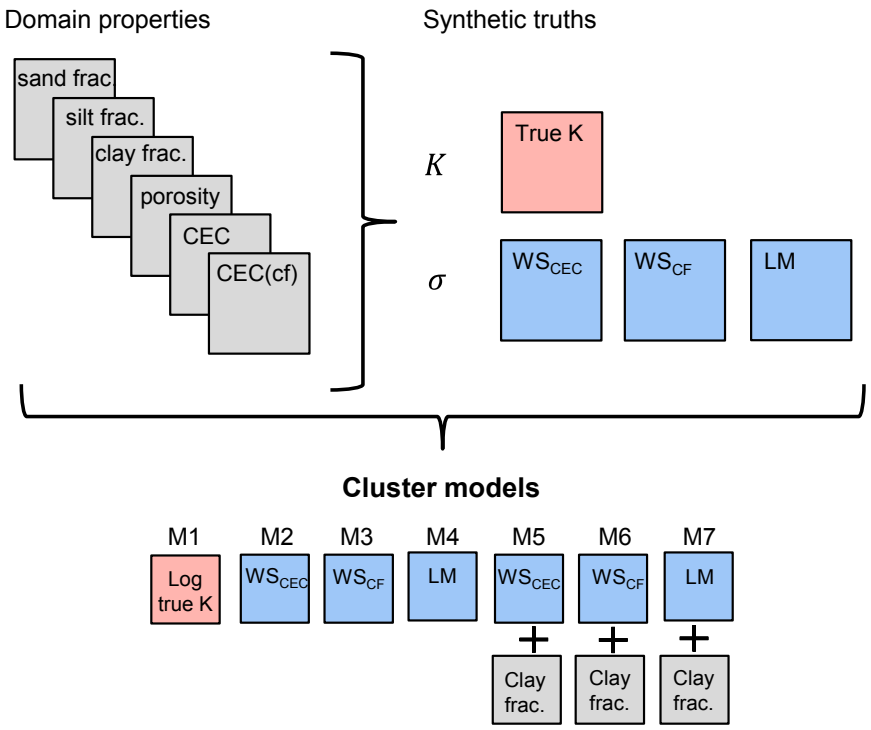

Figure 12 Illustration of how the three electrical conductivity synthetic truths, WS_{CEC}, WS_{CF}, and LM, and the true hydraulic conductivity have been constructed. The connection and input to the seven cluster models M1 to M7 is also shown.

The structures of the synthetic domain are multi-modal Gaussian, and they were created using random Gaussian fields. The properties of the domain were obtained partly from 21 soil samples, which have been previously characterized in other studies, in order to obtain a realistic relationship between clay fraction and CEC. The structural domain was populated with soils corresponding to mixtures of the 21 soil samples. The reader is referred to section 2.1 and section 2.2 respectively of Paper **II** for a full description of how the structures and the properties of the domain were constructed. The domain properties, see Figure 12, are used as input to models for K and σ. True K is modeled using the model proposed by Revil and Cathles (1999). A simple linear mixing model (Beamish, 2013) was used to model the LM σ synthetic truth. The two other σ synthetic truths, WS_{CEC} and WS_{CF}, were modeled using the model presented by Waxman and Smits (1968), WS_{CEC} using CEC to estimate surface electrical conductivity and WS_{CF} using clay fraction to estimate surface electrical conductivity.

Seven cluster models are constructed as shown in Figure 12. M1 is the cluster model obtained from clustering on true log K, which is used as a reference to evaluate the hydrological performance.

4.5 Hydrological models, calibration and predictions

The hydrological models used for the synthetic study, Norsminde and Kasted are briefly presented here. For details the reader is referred to Paper **II**, Paper **III** and Paper **IV** respectively.

A sketch of the synthetic groundwater flow model is shown in Figure 13. It is a steady state MODFLOW2000 model comprising of 100 by 100 10 m grid cells and 1 layer. Water flows diagonally from the constant head boundary of 100 m to the constant head boundary of 90 m. The pump in the center of the domain is not active during calibration, but used for predictions only. 15 head observations and 1 flow observation, generated from a forward run of the true *K* field, are utilized in the calibration. Pumping well capture isochrones are used as hydrological predictions, which are calculated using the 'stream2' and 'interpstreamspeed' functions in MATLAB2014b.

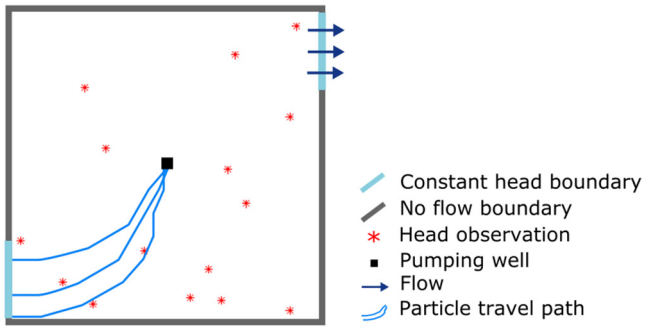

Figure 13 Synthetic groundwater flow model

The hydrological model for the Norsminde site is a transient integrated hydrological model setup using the MIKE-SHE code. The model is created as a refined and extended version of the DK-model (Henriksen et al., 2003) of the same area. The DK-model is a national groundwater resource model for Denmark. The numerical grid is 180 by 160 of 100 m large cells in the horizontal. The groundwater model consists of 37 numerical layers covering from 100 mamsl to -120 mamsl, of which the uppermost layer is 10 m thick and the remaining layers are 4 m thick. The parameterization is described in section 2.3.1 in Paper **II**. Data available for calibration amount to hydraulic head observations from 132 wells (point or time series) and daily stream discharge time series at three gauging stations translated from water level observations.

The groundwater model for the Kasted site is a steady-state MODLFOW-USG model (Panday et al., 2015). The numerical grid is 232 by 136 of 50 m cells in the horizontal and 11 vertical layers of varying thickness. Surface near layers follow and even out topography and deeper layers approach a more horizontal orientation. The uppermost layers are between 10 m and 20 m thick and the deeper layers are between 5 m and 10 m thick. Calibration data comprises of 94 steady state hydraulic head observations and three sub-catchment base-flow estimates. Well catchment areas are calculated using mod-PATHDU (Muffels et al., 2014) by backward tracking 1,000 particles from cylinder shaped seeding volumes from model grid cell containing the pumping well.

4.6 Probabilistic prediction from uncertain K structure

In Paper **IV** the cluster approach is extended to generate stochastic hydrostratigraphical models. A probabilistic ensemble of hydrostratigraphical cluster models was created for the Kasted site. The uncertainty represented in the ensemble is the uncertainty due to data gaps only: resistivity data and clay-fraction values are assumed certain and thus used deterministically. The K value of each cluster in each realization is estimated in the hydrological inversion.

The ensemble of hydrostratigraphical models and groundwater model predictions is obtained in the following way:

1. Clay-fraction inversion yields spatially coinciding resistivity data and clay-fraction values, scattered in x and y
2. k-means clustering on principal components of normalized resistivity data and clay-fraction values
3. Fit of indicator variogram model to sample indicator variogram of each cluster
4. Simulate realization of clusters (i.e. categories) using sequential indicator simulation (SIS) onto 3-D regular grid
5. Estimate cluster K values in hydrological model calibration
6. Particle tracking for selected pumping wells
7. Combine prediction from each realization results in a probabilistic prediction

Step 4 to step 6 is repeated for each of the 75 realizations.

The ensemble of hydrostratigraphical models is obtained using a two-point geostatistical indicator approach. The probability of occurrence of a cluster separated by a distance h is described by its sample indicator semivariance $\gamma_s(h)$:

$$\gamma_s(h) = \frac{1}{2N(h)} \sum_{i}^{N(h)} (I(i) - I(i+h))^2 \qquad (6)$$

where $I(i)$ is the indicator value at point i and $N(h)$ is the number of observation pairs for the separation distance h. I.e. "the indicator variogram value $2\gamma_s(h)$ measures how often two locations a distance h apart belong to different categories" (Goovaerts, 1997). The 3-dimensional connectivity is represented using horizontal and vertical variograms. Experimental variograms were calculated for 8 directions in the horizontal *xy*-plane, which confirmed that isotropic horizontal variograms can be used.

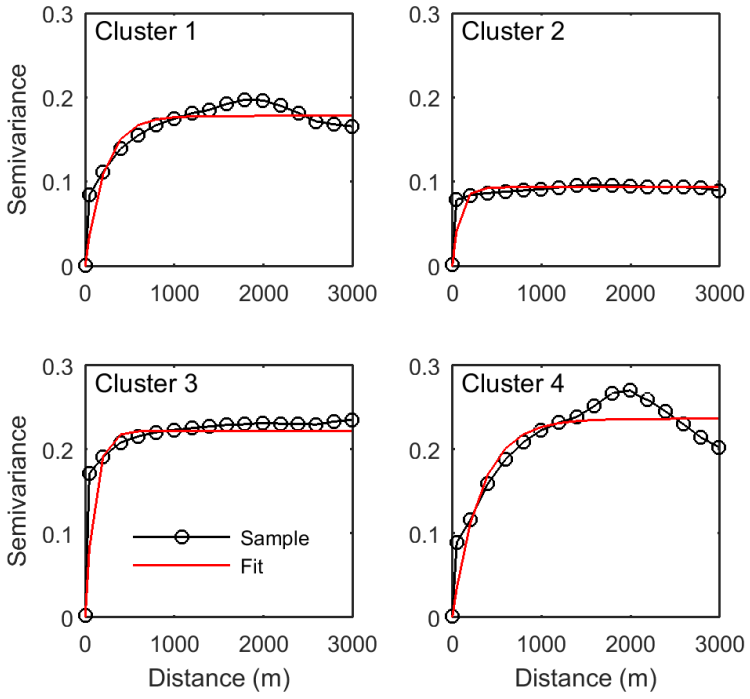

Figure 14 Sample (black dots and line) and modeled (red line) indicator variograms for the 4-cluster case.

Sequential indicator simulation (SIS) (Gómez-Hernández and Srivastava, 1990) implemented in GSLIB (Deutsch and Journel, 1998) has been used to make the cluster model realizations. The steps of SIS algorithm are:

1. Define random path visiting each grid node in the simulation grid
2. At each grid node the probability of each cluster is determined from the indicator variogram models. The probabilities are conditional to data and all other previously simulated nodes.
3. A cumulative distribution function is built from the conditional probabilities, and by drawing a random number between 0 and 1 a cluster is simulated at the grid node.
4. The simulated grid node is added to the conditioning data set, and the next grid node is visited.

The use of geophysical data in geostatistics poses the potential issue of over-conditioning due to the spatially correlated geophysical data (Koch et al., 2014). This problem is automatically solved by representing geophysical and borehole information with clusters.

5 Software and computations

The computations used to produce the results for this PhD work was completed through the use of several open source and licensed software. A list of the software including website for download (when possible) can be found in Table 3.

Hydrological models were setup using the codes: MIKE-SHE for Norsminde, MODFLOW-USG for Kasted, and MODFLOW-2000 in the synthetic study. Hydrological inversion of the three models were performed with PEST.

Well-capture zone predictions at Kasted and mean travel time predictions in the synthetic model were computed using mod-PATH3DU (Muffels et al., 2014) and MODPATH-5 respectively.

The sequential indicator simulation algorithm, SISIM, was run as command line executable. The book "GSLIB: Geostatistical Software Library and User's Guide" (Deutsch and Journel, 1998), which serves as a manual for all programs included in GSLIB, was used in order to setup the simulation configuration file.

k-means cluster analysis was completed in the MATLAB2012b and MATLAB2014b implementation in the '*kmeans*' function (Arthur and Vassilvitskii, 2007; Lloyd, 1982).

5.1 Computation time

Local calculation servers installed with Microsoft operating systems were used to perform the computations, and a small part of the computations were performed on the Linux cluster operated by DCC, the high performance computing center at the Technical University of Denmark. Computation jobs were executed at the Linux cluster through a queuing system accessed through a ssh connecting. Local calculation servers are accessed through a remote desktop connection and computation jobs are managed through a spreadsheet booking system. Four local servers each with 32 multithreaded CPUs or similar were available and shared among the research community at the Department of Environmental Engineering. Hydrological model inversion, *k*-means analysis, variogram modeling, and SISIM simulations were performed with these resources.

Utilizing parallelization onto 10 threads, calibration of the transient Norsminde MIKE-SHE model took 1 day for a 2-cluster case, 3 days for a 5-

cluster case, and between 3 and 5 days for calibration of larger number of clusters. MIKE-SHE automatically parallelizes onto four threads if available (i.e. a calibration typically benefitted from 40 threads). With four threads available one model forward run took 45 minutes. The inversion for the Norsminde model is computed on an Intel® Xeon® CPU E7-4830 2.13GHz (4 processors) 16 multithreaded cores (= 64 CPUs), 64GB RAM or similar, installed with Windows Server 2008 R2 Enterprise.

Utilizing parallelization onto 8 threads, calibration of the steady state Kasted MODFLOW-USG model took 50 minutes for a 2-cluster case, 1 hour for the 4-cluster case, and between 2 and 3 hours for 7- and 8-cluster cases. A forward model run takes approximately one minute. The inversion for the Kasted model is computed on a Intel® Xeon® CPU E5-2698 v3 2.30GHz (2 processors) 32 multithreaded cores (= 64 CPUs), 128GB RAM or similar, installed with Windows Server 2012 R2 Standard.

All calibrations were parallelized using BEOPEST. Computational times vary with the number of calibration parameters, numerical convergence of forward models, and convergence of the inverse problem.

For the Norsminde site clustering was performed in the regular grid consisting of 1,584,000 grid cells (180 x 160 x 55). A large part of the domain representing the Paleogene clay was not considered during clustering. Depending on the number of clusters the 200 replicates took from 15 minutes for a 4-cluster case to more than an hour for the 8-cluster model. The computations were done on the same local Windows server as the Norsminde calibrations.

For the Kasted site clustering was performed on *xy* scattered data at 284,542 point locations. The computation time to obtain the 200 replicates depend on the number of cluster; a 2-cluster case took 4 minutes, a 4-cluster case took 6 minutes and a 8-cluster case took 16 minutes. The computations were performed on one node on the Linux clusters.

The automatic fitting routine available in the R package “gstat” (Pebesma, 2004) used to fit cluster variograms for the Kasted site was run on the Linux clusters (one process/node). For each cluster in each of the cluster models, the fitting routine uses binary information of the scattered data points. Fitting variograms for the 2 clusters in the 2-cluster case took 13 minutes, fitting variograms for the 4 clusters in the 4-cluster case took 22 minutes and fitting variograms for the 8 clusters in the 8-cluster case took 48 minutes.

SIS simulation with of 284,542 scattered data points onto a regular grid of 1,198,976 grid cells was performed on the local Windows servers. Due to the size of the output text files the 100 realizations were simulated in two rounds of each 50 realizations. The size of an output file containing 50 realizations is 1 GB. SISIM cannot be parallelized by running the program from several command lines simultaneously. Simulation of 50 realizations using one node/process the 2-cluster case took 20 minutes, the 4-cluster case took 39 minutes and the 8-cluster case took 2 hours and 4 minutes.

Table 3 List of software used for the work presented in this PhD. Software for inversion of EM data and clay-fraction inversion is not included.

Software	Open	Access	Manual	Purpose
MIKE-SHE	no	-	online	GW forward model
MODFLOW-USG	yes	http://water.usgs.gov/ogw/modflow/	online	GW forward model
MODFLOW-2000	yes	http://water.usgs.gov/ogw/modflow/	online	GW forward model
Mod-PATH3DU	no	-	online	GW model prediction
PEST	yes	http://www.pesthomepage.org/Downloads.php	online	GW model calibration
BEOPEST	yes	http://www.pesthomepage.org/Downloads.php		Parallelization of PEST
SISIM (gslib)	yes	http://www.statios.com/GSLIB/index.html	book	Sequential indicator simulation
gstat (R)	yes	https://cran.r-project.org/web/packages/gstat/index.html	online	Variogram models fitting / Gaussian field generation
MATLAB2014b	no	-	online	*k*-means clustering, general data analysis and plotting, streamline calculations
Python 2.7.11	yes	https://www.python.org/downloads/	online	Data parsing
GeoScene3D	no	-	-	Visualization of 3-D models (hydrostratigraphy, resistivity, clay fraction)
ArcGIS	no	-	-	2-D visualization of data and maps

6 Summary of main results

This results section summarizes the main findings of the results presented in Papers **I-IV**. The main results for the PhD work are:

- Clustering on σ and clay-fraction results in structures for which hydrological model K values can be determined. Corresponding hydrological predictions are comparable to the true predictions.
- We can build 3-dimensional groundwater model hydrostratigraphy directly from AEM resistivity data and borehole lithological information.
- The method is data-driven, objective and reproducible.
- The hydrological performance of the cluster model-based groundwater model is competitive with comparable groundwater resource models.
- The parsimonious number of clusters to represent subsurface structures can be guided by the hydrological data and model.
- The ensemble of hydrostratigraphical cluster models can be used to address groundwater model prediction uncertainty.

The major findings shown in the bullets will be presented in the following. First insight gained from the synthetic study will be presented (Paper **II**). Second the results for the construction of the hydrostratigraphical cluster models will be presented from resistivity and clay-fraction values to 3-D cluster model (Paper **I**, Paper **III** and Paper **IV**). Third the hydrological performance of the deterministic models from Norsminde and Kasted will be compared to that of similar groundwater resource models. Fourth probabilistic cluster and hydrological results are presented in terms of uncertain hydrostratigraphical models and the resulting uncertain well catchment areas.

6.1 Synthetic study

Exploiting the existence of a true *K* field Paper **II** presents a synthetic case to investigate for which cases the cluster approach is or is not valid.

The main findings in Paper **II** are illustrated in Figure 15. Figure 15 shows the hydrological performance, in terms of fit to calibration data (a) and reproducing a pumping well capture isochrone (b) of all seven models, M1 to M7. For every model 1-cluster to 8-cluster cases are calculated, as shown in Figure 15. The isochrone fit is shown as percentage of overlap with the true isochrone, calculated from the heterogeneous *K* field. From a 4-cluster case and on all three petrophysical relationships are able to reproduce hydrological prediction if clay fraction is included in the cluster analysis (see M5, M6, and

M7). The cyan (M2) and gray (M4) dashed lines, representing cluster models based on electrical conductivity only, do not stabilize but continue to fluctuate beyond the 4-cluster case. Interestingly, if σ is corrected for the effect CEC, clustering on σ alone (M3) produce similar results as when including clay fraction in the cluster analysis.

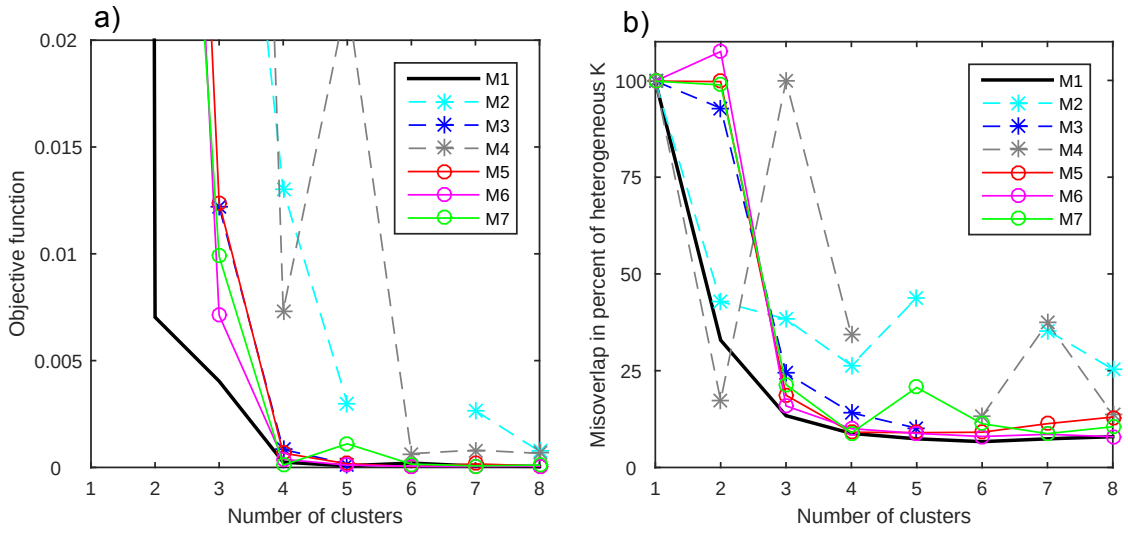

Figure 15 a) Fit to calibration data. b) Areal mismatch in percent between the area represented by the well capture isochrone from the true *K* field and the area represented by the well capture isochrone from the cluster models of varying number of clusters. Models M1 to M7 are shown for the 1- to 8-cluster cases.

One interesting observation made in Paper **II** was how different the cluster models can be, while producing similar results in terms of hydrological performance. Figure 16 has been included to show this using the models M5 and M7, and M2 is included to show an example of how clustering on σ is not sufficient. The difference in how M5 and M7 discriminate log *K* values is visible from Figure 16 'M5' and 'M7', especially cluster 2 and cluster 3. This results in large structural differences, as the lower panel in Figure 16 illustrates. The estimated log *K* values, see Table 4, differ; cluster 1 and cluster 2 have the same *K* value in M5, whereas the *K* values of M7 are different from each other. In terms of hydrological predictive capability M5 and M7 perform equally well.

Table 4 Calibrated log *K* (m/s) values for the 4-cluster case of all seven models. M2, M5, and M7 are highlighted.

	Cluster 1	Cluster 2	Cluster 3	Cluster 4
M1	-5.01	-5.73	-6.52	-7.53
M2	-4.84	-5.01	-5.65	-7.41
M3	-4.99	-5.00	-5.97	-7.44
M4	-4.76	-5.73	-6.35	-9.00
M5	-4.95	-4.98	-6.10	-7.36
M6	-4.93	-5.29	-6.11	-7.35
M7	-4.96	-5.65	-6.47	-7.53

The inability of the M2 model to discriminate log *K* values (see large overlaps in Figure 16 'M2') results in an erroneous delineation of the well catchment isochrone. The fit to calibration data show a similar disagreement.

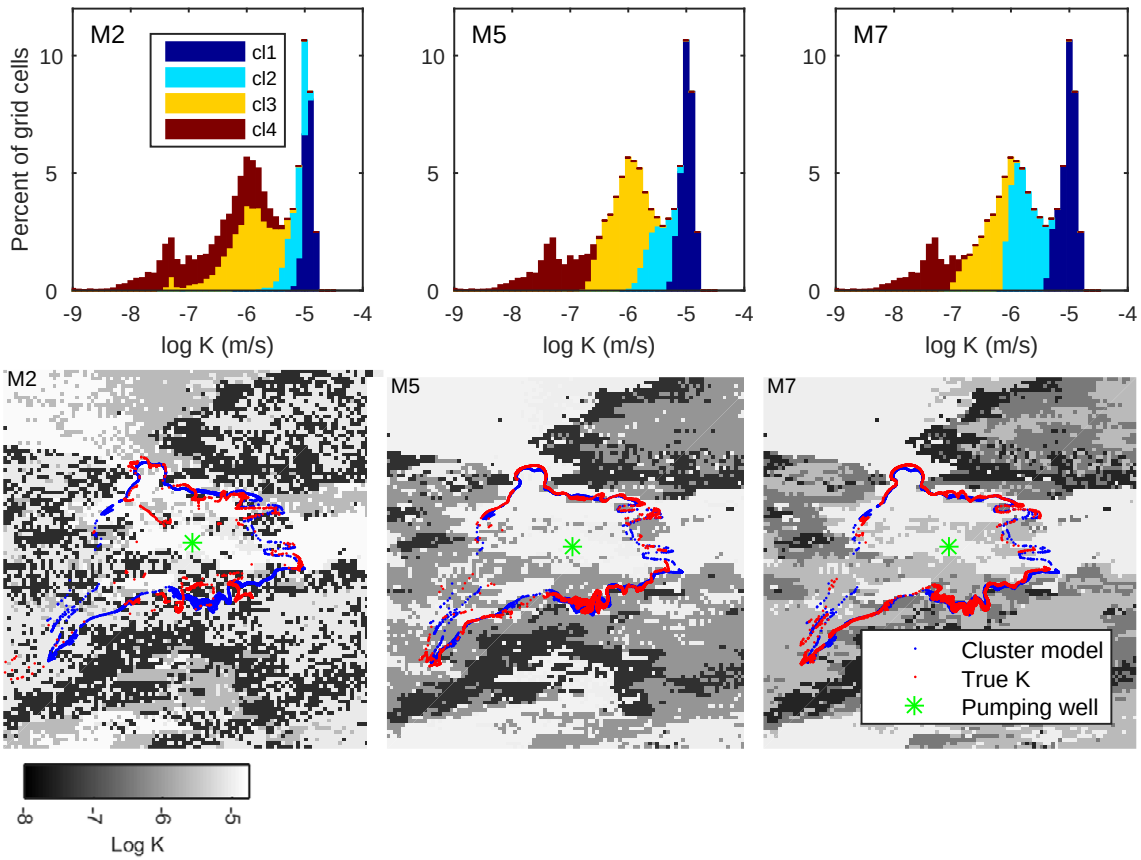

Figure 16 Models M2, M5, and M7 shown in terms of how each model discriminates log *K* values (upper panel) and the calibrated *K* field and predicted well catchment isochrones (lower panel).

6.2 Cluster model hydrostratigraphy

The construction of the deterministic hydrostratigraphical cluster models for Norsminde and Kasted are illustrated in Figure 17 and Figure 18 respectively.

The hydrostratigraphy for Norsminde is built from the resistivity model and clay-fraction model shown in box A in Figure 17. The 2-dimensional value space formed by resistivity and clay-fraction values is subdivided into five clusters (box B). The colors of the scatter plots indicate logarithmic data density; a value of two thus corresponds to 100 grid cells. The histograms show how the resistivity models and clay-fraction values are represented in the five clusters, in percentage of the total number of grid cells. Box C is the 3-dimensional domain obtained by replacing the grid cells by the cluster values determined in box B.

Figure 17 indicates how the hydrostratigraphy is obtained directly from the two inversion products, the resistivity model and the clay-fraction model. However, the two 3-D models shown in box A in Figure 17 are obtained by kriging resistivity models and clay-fraction values from the geophysical sounding sites onto a regular 3-D grid, resulting in smoothed models. The smoothness of the 3-D resistivity grid is visible in box A, which results in 'onion ring' shapes in the cluster model in box C. The intersection of the Boulstrup valley, which is shown in the 3-D grids, shows the 'onion ring' trend. Cluster interfaces occur as transition zones. The transition from cluster 1 to cluster 5 to occurs, to a large extent, first by a transition to cluster 2, then 3, then 4. Cluster 1 never neighbors cluster 5. This is especially true for the tunnel valleys. In some areas cluster 1 transitions directly to cluster 3 or cluster 4. The 'onion ring' tendency is a problem because it is a clear artefact. Kriging replaces the cognitive spatial interpretation made by a geologist.

To avoid the 'onion rings', interpolation to a regular 3-D grid was obtained by using the mode model instead of the mean model at the Kasted site. The steps are shown in Figure 18. Box C shows how the 'onion rings' are no longer present and transition occurs between all clusters. This is seen in the tunnel valleys shown in the horizontal slice and in the profile in box C.

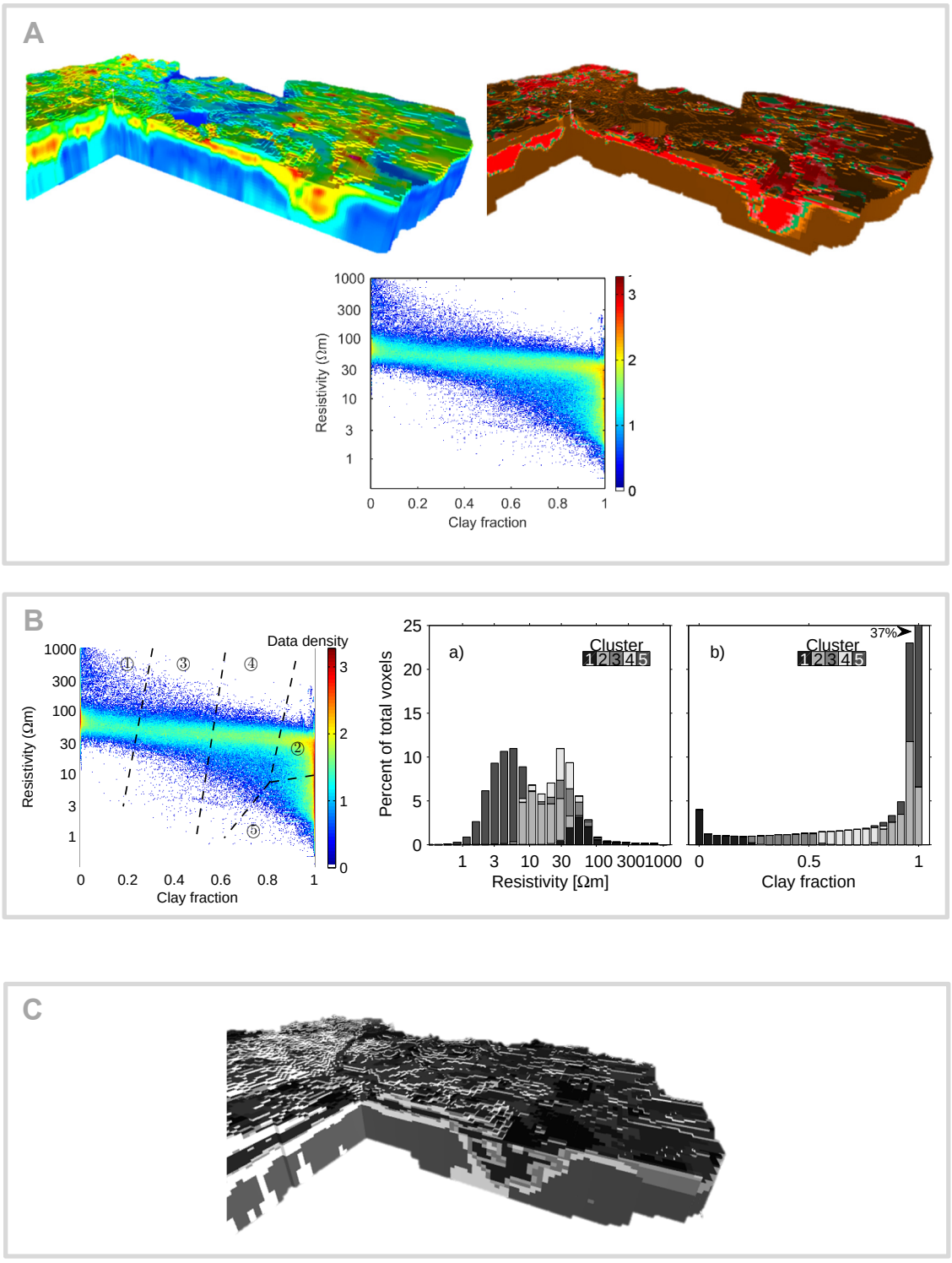

Figure 17 Illustration of the clustering approach applied to Norsminde. A Input, resistivity model and clay-fraction values in a regular grid; B Cluster analysis; C The resulting hydrostratigraphical model.

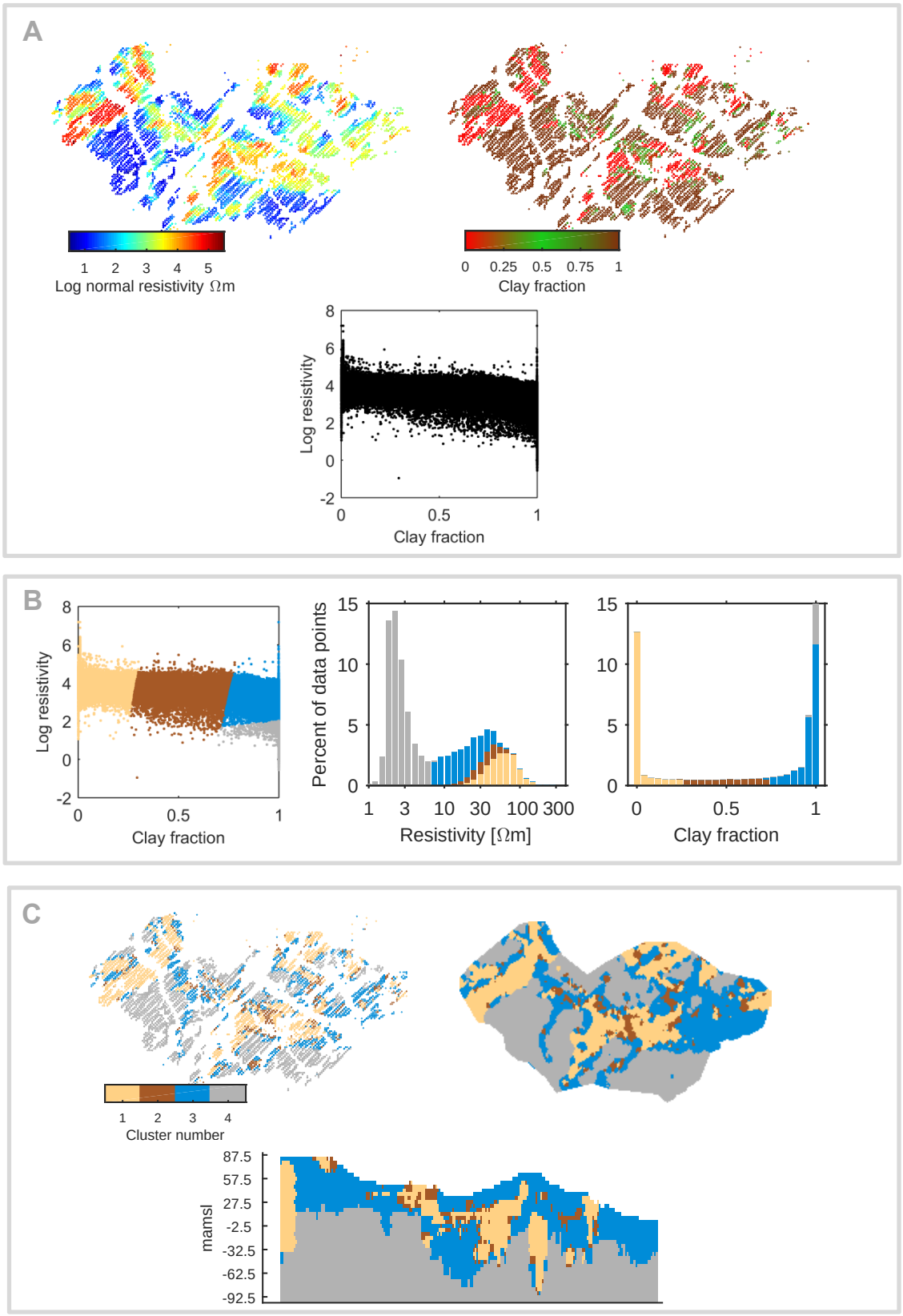

Figure 18 Illustration of the cluster approach applied to Kasted. A Input, resistivity models and clay-fraction values; B Cluster analysis; C The resulting hydrostratigraphical model.

6.3 Hydrological performance

Table 5 summarizes cluster characteristics for the 5-cluster model at Norsminde and the 4-cluster mode model at Kasted. The table shows mean, minimum and maximum values. The estimated hydraulic conductivity values obtained by calibration are also presented.

Table 5 Cluster characteristics in terms of resistivity, clay-fraction, and estimated hydraulic conductivity. N is Norsminde and K is Kasted.

Cluster #		Log resistivity [Ωm] mean (min/max)		Clay fraction mean (min/max)		Hydraulic conductivity [ms^{-1}]	
N	K	N	K	N	K	N	K
1	1	4.3 (1.3/7.1)	4.2 (1.1/7.2)	0.083 (0/0.30)	0.041 (0.0020/0.30)	4.40E-04	7.66E-05
3	2	3.8 (0.22/6.9)	3.6 (-0.95/5.5)	0.42 (0.21/0.61)	0.53 (0.26/0.78)	2.36E-07	4.15E-05
4	3	3.4 (-0.25/6.5)	3.0 (1.8/7.2)	0.71 (0.52/0.89)	0.97 (0.72/1.0)	1.34E-08	1.49E-07
2	4	2.9 (2.0/6.2)	1.0 (-0.55/2.0)	0.97 (0.81/1.0)	1.0 (0.70/1.0)	6.28E-09	1.00E-09
5	-	1.5 (-1.5/2.2)	-	0.99 (0.65/1.0)	-	5.98E-08	-

The decision for the parsimonious number of clusters with which to represent the subsurface was judged from the hydrological data and model. We want to use a hydrostratigraphical model that explains the hydrological data with the lowest number of free parameters as possible. Figure 19 shows the parsimonious plots for a) Norsminde and b) Kasted. For Norsminde the mean standard deviation of the log *K* values across the clusters was included in the plot (blue line). The plots indicate that a 3-cluster to 5-cluster model is optimal for Norsminde, while a 4-cluster model is optimal for Kasted.

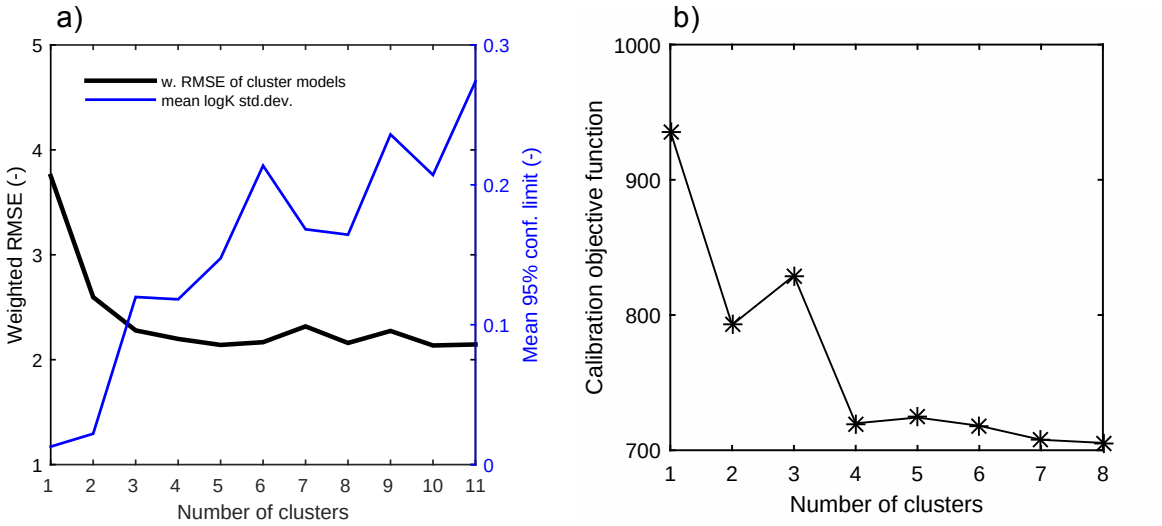

Figure 19 Choice of number of clusters to represent the subsurface. a) Norsminde, weighted RMSE for head as a function of the number of clusters, and b) Kasted, objective function as a function the number of clusters.

Calibration statistics are presented in **Table 6**. The calibration of the transient Norsminde model resulted in a root mean square error (RMSE) for simulated hydraulic head of 2.0 m and a mean error (ME) of -0.79 m. In Paper **III** these results were found satisfactory by benchmarking against performance statistics of comparable Danish hydrological models. RMSE for the simulated hydraulic heads from the steady state model at Kasted is 5.5 m and the ME is -0.81 m. The markedly higher RMSE is because seasonal dynamics are not captured by the steady state model. Observed head is plotted against simulated head in Figure 20.

Table 6 Calibration statistics for the Norsminde and Kasted models

	Norsminde 5 clusters		Kasted 4 clusters	
	Head (m)	Discharge (m^3/s)	Head (m)	Base flow (percent)
RMSE	2.0	0.28	5.5	-
ME	-0.79	-0.011	-0.81	-
Percent error	-	-	-	1.6

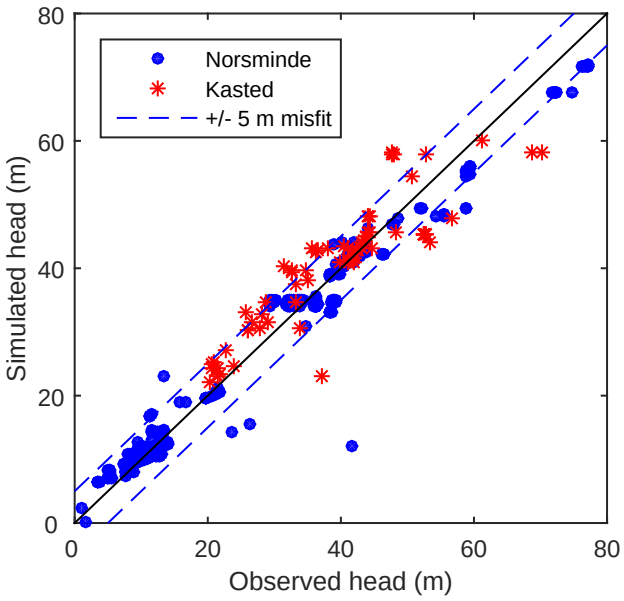

Figure 20 Observed head versus simulated head for Norsminde and Kasted. A 5 meter misfit is indicated with dashed blue lines.

6.4 Uncertain well catchment area due to uncertain hydrostratigraphy

The probabilistic analysis was performed using 75 realizations of the subsurface hydrostratigraphy of the Kasted site. The probability of each of the clusters at a given location is shown in Figure 21 and Figure 22.

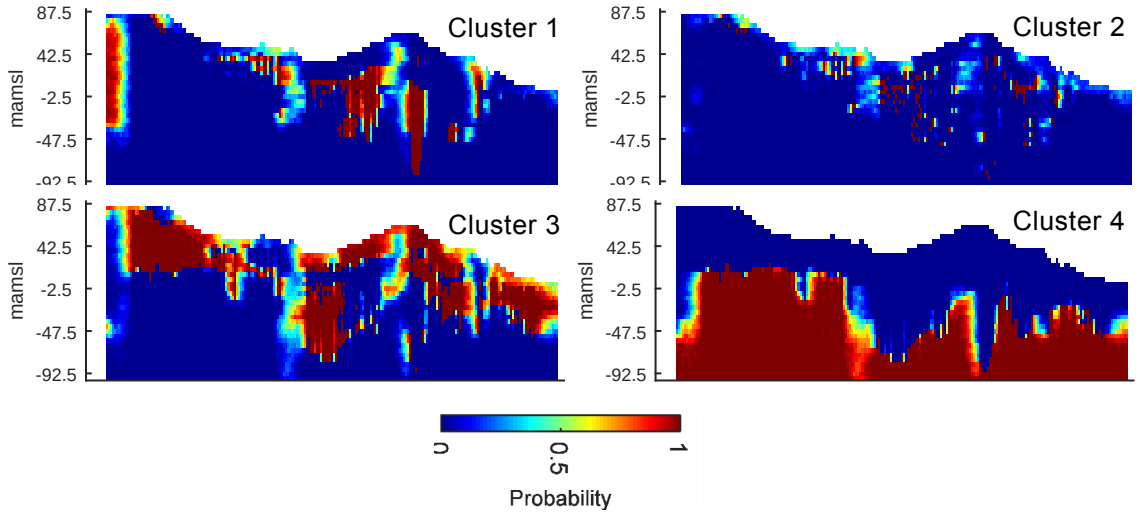

Figure 21 Probability map of the spatial distribution of the four clusters. West-East trending profile through the center of the domain.

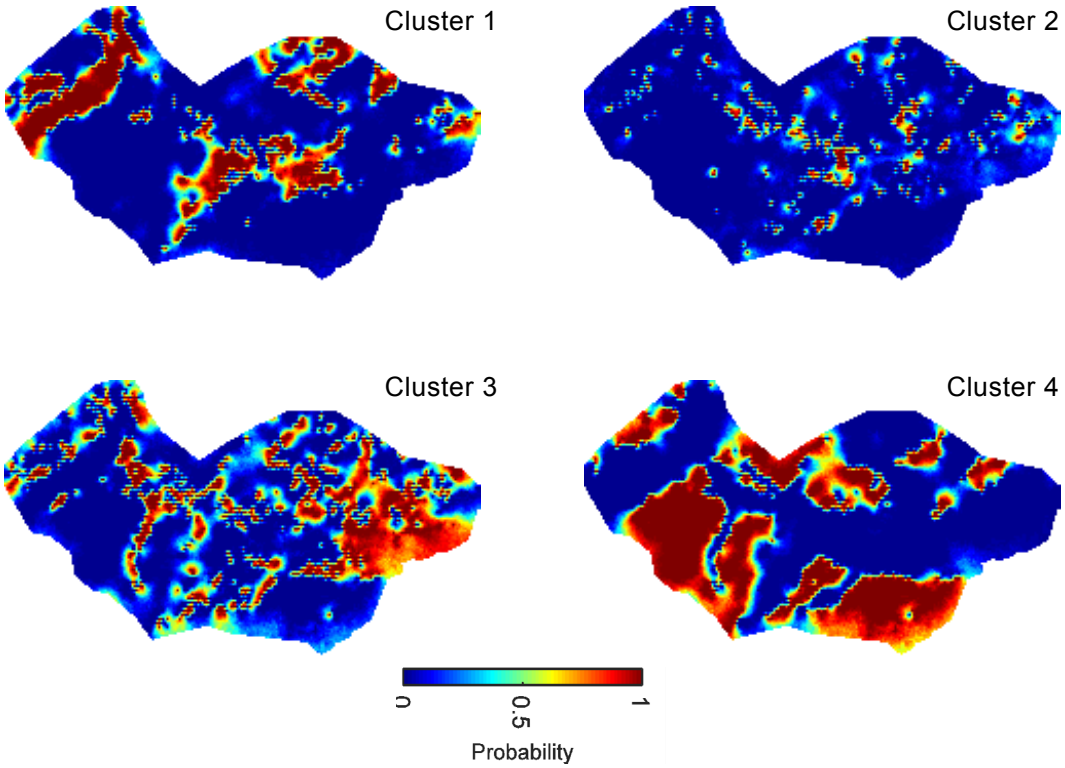

Figure 22 Probability map of the spatial distribution of the four clusters. Horizontal 5 meter interval at 2.5 mamsl.

The probabilistic cluster maps give an impression of the structural differences represented by the hydrostratigraphical ensemble. Dark red areas are well determined by data. The main geological features are determined by the available data. Structural uncertainty thus is indicated by colors of light blue, green and yellow. The structural uncertainty represents local scale variations, which is also illustrated by maps of eight realizations in Paper **IV**. The figures show how the interfaces between the hydrostratigraphical units (i.e. the clusters) are uncertain.

The structural uncertainty shown in Figure 21 and Figure 22 translates into the uncertain delineation of the well catchment area shown in Figure 23. The location of the focus area in Figure 23 is shown on the base map of Kasted (Figure 4). A value of 1 means that all realizations predict that a given grid cell belongs to the well catchment area. The pink star indicates the location of the pumping well. Green dots in panel b) represent the well catchment area predicted using a classically generated geological model. 85 percent of the realizations predict the well catchment area to extend towards the southwest.

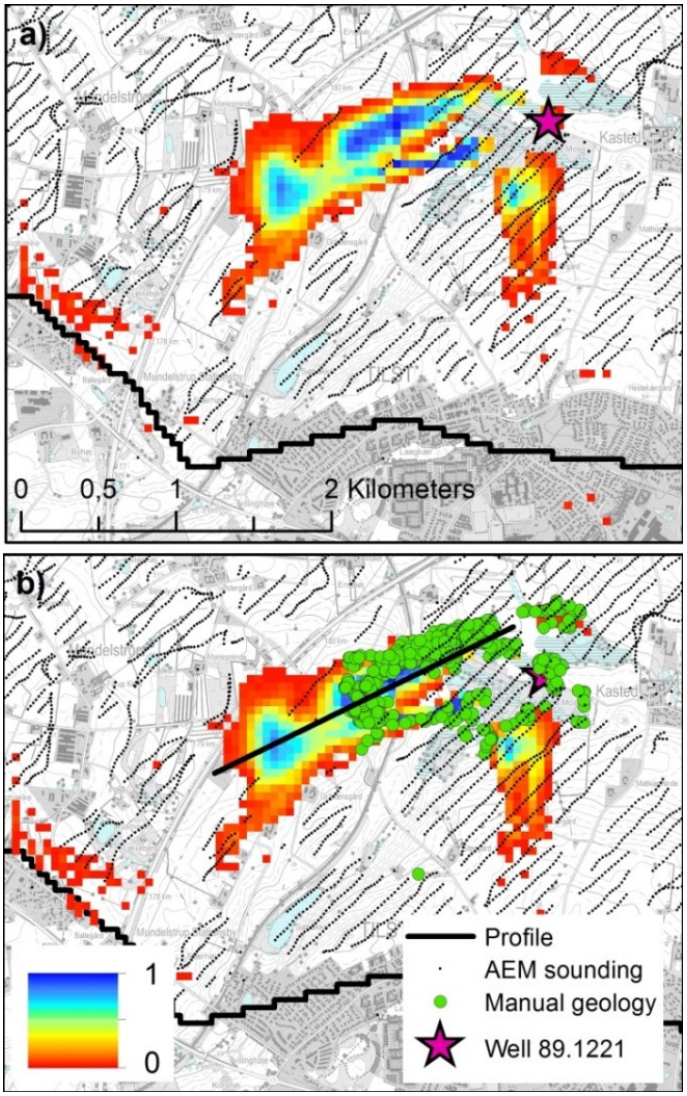

Figure 23 Probabilistic well catchment area for well 89.1221 of the Kasted well-field.

6.5 Limitations and advantages

Automation and data dependency makes the clustering approach objective and reproducible. All steps in the work flow can be documented, and the method is therefore independent of the person who performs the analysis. This is attractive in a groundwater management situation where new data may continuously be collected for a given site. The new data, be it geophysical, lithological and/or hydrological, can be immediately included in the modeling process resulting in an update of the groundwater model. The updates and version of data and model can be managed through log files and versioning software and code. Surely subjective choices have to be made, for example in the inversion of electromagnetic data and in the clay-fraction inversion.

These choices however can largely be documented, maintaining reproducibility.

Cognitive methods to map groundwater model hydrostratigraphy have the possibility of including several geophysical and geological data types, for example seismic data and geological maps and expert knowledge. However the uncertainty of these models - we know that they are uncertain - is not trivial to estimate. The reader is referred to Paper **III** 'Advantages and limitations' for a full discussion and comparison of automatic versus cognitive methods.

The clustering approach has been tested for a specific geological environment, namely glacially shaped unconsolidated sediments of sands, gravels, and tills overlying impermeable thick clays. Under different geological circumstances the approach is expected to perform differently, and for some geological environments the methods may not be applicable. Fundamentally, the electromagnetic method must be sensitive to the structural and lithological properties which are decisive for a groundwater flow system. Limestone aquifers, potentially fractured, for example represent very different flow systems. However, with modification, it is likely that the clustering approach can be altered in order to be applicable to a different geological environment, see section 8, 'Future research' for details.

7 Conclusions

The objective of this PhD was to study the use of airborne time-domain electromagnetic data and borehole lithological information to inform groundwater models.

A data-driven clustering approach to obtain groundwater model hydrostratigraphy from integration of AEM data and lithological information, which can be incorporated directly into the hydrological modeling process, has been proposed. Hydrostratigraphical units, formed as clusters in a cluster analysis, are assumed to have uniform hydrological properties, and the hydraulic conductivity of each unit is estimated in a groundwater model calibration constrained by hydrological observations.

A synthetic study was performed to evaluate how the method performs under three different electrical conductivity synthetic truths by comparing results with the true K field. Results show good agreement between the true well capture isochrones and isochrones obtained from clustering on electrical conductivity and clay fraction.

The clustering approach was successfully applied to two Danish field sites characterized by geology shaped by glacial activity, Norsminde and Kasted, respectively covering 156 km^2 and 46 km^2. At Norsminde the hydrological performance, in terms of fit to hydrological observations of head and stream discharge, was found satisfactory by benchmarking with comparable Danish hydrological models. The number of units in the hydrostratigraphical models to represent the subsurface was determined parsimoniously from the fit to hydrological observations.

Objectivity and reproducibility are key features of the work presented in this thesis. The clustering approach is largely data-driven. If new data is collected these can be directly incorporated, making the hydrostratigraphy continuously updated according to available data. On the contrary, the clustering approach may be inappropriate for sites where little data is available.

The second method builds on the clustering approach and utilizes geostatistical simulation based on indicator variograms in order to address the uncertainty of hydrological predictions originating from uncertain subsurface structures. An ensemble of equally likely hydrostratigraphical models was constructed, each assigned hydrological properties in the subsequent hydrological calibration. The 75 hydrostratigraphical models built for Kasted re-

sulted in a probabilistic well catchment area. Parts of the delineated catchment overlap with the catchment predicted using a classically generated geology, and results indicate an 85% probability that the well catchment area extends beyond. It was found that calibration data cannot identify the hydrostratigraphical realizations, that contribute to the large variations in terms of delineation of the well catchment area.

In conclusion, a direct integration of the large AEM data sets into hydrological models has been shown to be possible, when lithological information is included. Quantification of the subsurface structural uncertainty and its implications for hydrological predictions is unique, and the method can be used to aid management decisions under the knowledge of risk. Due to the fast construction of hydrostratigraphical models, the presented methods have commercial potential.

8 Future research

Here recommendations for potential future research in terms of method development and applications to other field sites are listed.

In terms of method development, the following is suggested:

- The clustering approach has been used by including two cluster variables only. However information about groundwater quality or geophysical data obtained from MRS soundings or IP methods can easily be incorporated into the cluster analysis. Groundwater quality data can differentiate between resistivity variations due to lithology and resistivity variations due to pore-water conductivity. This is of value in large areas with heterogeneous groundwater quality.
- Performing a weighted *k*-means analysis using the resistivity and clay-fraction value uncertainties was attempted during this PhD, however the work was not conclusive. The author recommends to further investigate how the uncertainty of cluster variables could be included in the clustering workflow.
- Elaborating on the uncertainty of the input data to the cluster analysis: the geostatistical simulation employed during this PhD work assumed that input data is error-free. The resistivity models and clay-fraction values determined during inversion however are uncertain. These uncertainties can be included in the probabilistic analysis by perturbing the resistivity models and clay-fraction values prior to the cluster analysis. A cluster analysis can be performed on each of the sets of perturbed resistivity and clay-fraction values, which are finally simulated onto a regular grid and used in the groundwater model calibration. The resulting probabilistic predictions are expected to be more uncertain, however it is unknown to what degree.

In terms of field site application that can potentially result in new insight or confirm/reject applicability to other situations:

- Norsminde and Kasted are geologically very similar, and the benefit of using electromagnetic data to aid mapping of hydrostratigraphy is well established for these geological settings. It would be interesting to investigate the applicability of the clustering approach in sites with a different geology.
- Salt water intrusion is a well-known problem in coastal regions in terms of drinking water quality. AEM data are currently used to delineate the

salt water intrusion fronts under the assumption that geological heterogeneity is negligible. Geological heterogeneity however can influence the dynamics of the salt water intrusion phenomenon. It might be possible to adapt the clustering approach to be applicable to salt water intrusion models, which would be of value to water management in such areas.

- Lastly, it would be interesting to study the data dependency of the clustering approach, given different hydrological scenarios. Norsminde and Kasted are both data-rich. Depending on the level of hydrostratigraphical detail needed to answer a given question and the data-density, the applicability of the clustering approach is expected to vary.

10 Glossary

Airborne electromagnetic data

Electromagnetic data collected using airborne systems flown for example with a helicopter. In this thesis it refers to airborne time-domain electromagnetic data. Abbreviated AEM.

Cation exchange capacity

The number of sites on mineral surfaces per weight occupied by cations and/or available for exchange with cations. Abbreviated CEC.

Clay fraction, synthetic study

Fraction of grains in soil sample with a diameter below than 2 μm.

Clay fraction, in clay-fraction inversion

Accumulated fraction of clay material (not clay mineral) over a given length interval. The vertical distribution is not specified.

Hydrostratigraphy

The three-dimensional distribution of geological material in the subsurface that is of relevance for groundwater flow and transport processes.

Petrophysical relationship

Mathematical relationship between a geophysical property and a hydrological property.

Pore-water electrical conductivity

Contribution to the bulk electrical conductivity of a porous material that is due to flow of currents in the water-filled pore space (here saturated). Abbreviated σ_w.

Surface electrical conductivity

Contribution to the bulk electrical conductivity of a porous material that is due to the flow of currents on the grain surfaces. Abbreviated σ_s.

Well catchment area

The area on the land surface from where water recharges to a pumping well.

11 References

Aeschbach-Hertig, W. and Gleeson, T.: Regional strategies for the accelerating global problem of groundwater depletion, Nat. Geosci., 5(12), 853–861, doi:10.1038/ngeo1617, 2012.

Archie, G. E.: The electrical resistivity log as an aid in determining some reservoir characteristics, Trans. Am. Inst. Min. Metall. Eng., 146, 54–61, 1942.

Arthur, D. and Vassilvitskii, S.: k-means plus plus : The Advantages of Careful Seeding, Proc. EIGHTEENTH Annu. ACM-SIAM Symp. Discret. ALGORITHMS, 1027–1035, 2007.

Auken, E. and Christiansen, A. V: Layered and laterally constrained 2D inversion of resistivity data, Geophysics, 69(3), 752–761, doi:10.1190/1.1759461, 2004.

Auken, E., Christiansen, A. V., Westergaard, J. H., Kirkegaard, C., Foged, N. and Viezzoli, A.: An integrated processing scheme for high-resolution airborne electromagnetic surveys, the SkyTEM system, Explor. Geophys., 40(2), 184, doi:10.1071/EG08128, 2009.

Barfod, A. A. S., Møller, I. and Christiansen, A. V: Compiling a national resistivity atlas of Denmark based on airborne and ground-based transient electromagnetic data, J. Appl. Geophys., 2016.

Beamish, D.: The bedrock electrical conductivity structure of Northern Ireland, Geophys. J. Int., 194(2), 683–699, doi:10.1093/gji/ggt073, 2013.

Bedrosian, P. A., Maercklin, N., Weckmann, U., Bartov, Y., Ryberg, T. and Ritter, O.: Lithology-derived structure classification from the joint interpretation of magnetotelluric and seismic models, Geophys. J. Int., 170(2), 737–748, doi:10.1111/j.1365-246X.2007.03440.x, 2007.

Beven, K. and Binley, A.: The future of distributed models: Model calibration and uncertainty prediction, Hydrol. Process., 6(3), 279–298, doi:10.1002/hyp.3360060305, 1992.

Beven, K. and Binley, A.: GLUE: 20 years on, Hydrol. Process., 28(24), 5897–5918, doi:10.1002/hyp.10082, 2014.

Binley, A., Hubbard, S. S., Huisman, J. A., Revil, A., Robinson, D. A., Singha, K. and Slater, L. D.: The emergence of hydrogeophysics for improved understanding of subsurface processes over multiple scales, Water Resour. Res., 51(6), 3837–3866, doi:10.1002/2015WR017016, 2015.

Borden, D.: Baseline Studies of the Clay Minerals Society Source Clays: Cation Exchange Capacity Measurements by the Ammonia-Electrode Method, Clays Clay Miner., 49(5), 444–445, doi:10.1346/CCMN.2001.0490510, 2001.

Bosch, J. H. A., Bakker, M. A. J., Gunnink, J. L. and Paap, B. F.: Airborne electromagnetic measurements as basis for a 3D geological model of an Elsterian incision
[Hubschrauberelektromagnetische Messungen als Grundlage für das geologische 3D-Modell einer glazialen Rinne aus der Elsterzeit], Zeitschrift der Dtsch. Gesellschaft für Geowissenschaften, 160(3), 249–258, doi:10.1127/1860-1804/2009/0160-0258, 2009.

Carle, S. F. and Fogg, G. E.: Transition probability-based indicator geostatistics, Math. Geol., 28(4), 453–476, doi:10.1007/BF02083656, 1996.

Cassiani, G. and Binley, A.: Modeling unsaturated flow in a layered formation under quasi-steady state conditions using geophysical data constraints, Adv. Water Resour., 28(5), 467–477, doi:10.1016/j.advwatres.2004.12.007, 2005.

Chongo, M., Christiansen, A. V., Fiandaca, G., Nyambe, I. A., Larsen, F. and Bauer-Gottwein, P.: Mapping localised freshwater anomalies in the brackish paleo-lake sediments of the Machile–Zambezi Basin with transient electromagnetic sounding, geoelectrical imaging and induced polarisation, J. Appl. Geophys., 123, 81–92, doi:10.1016/j.jappgeo.2015.10.002, 2015.

Christiansen, A. V, Auken, E. and Sorensen, K.: The transient electromagnetic method, in Groundwater Geophysics - a Tool for Hydrogeology, edited by R. Kirsch, Springer, Berlin., 2006.

Christiansen, A. V., Foged, N. and Auken, E.: A concept for calculating accumulated clay thickness from borehole lithological logs and resistivity models for nitrate vulnerability assessment, J. Appl. Geophys., 108, 69–77, doi:10.1016/j.jappgeo.2014.06.010, 2014.

Delhomme, J. P.: Spatial variability and uncertainty in groundwater flow parameters: A geostatistical approach, Water Resour. Res., 15(2), 269–280, doi:10.1029/WR015i002p00269, 1979.

Deutsch, C. and Journel, A. G.: GSLIB: Geostatistical Software Library and User's Guide, Oxford University Press., 1998.

Deutsch, C. V.: A sequential indicator simulation program for categorical variables with point and block data: BlockSIS, Comput. Geosci., 32(10), 1669–1681, doi:10.1016/j.cageo.2006.03.005, 2006.

Dickson, N. E. M., Comte, J.-C., Renard, P., Straubhaar, J. A., McKinley, J. M. and Ofterdinger, U.: Integrating aerial geophysical data in multiple-point statistics simulations to assist groundwater flow models, Hydrogeol. J., 23(5), 883–900, doi:10.1007/s10040-015-1258-x, 2015.

Doetsch, J., Linde, N., Coscia, I., Greenhalgh, S. A. and Green, A. G.: Zonation for 3D aquifer characterization based on joint inversions of multimethod crosshole geophysical data, Geophysics, 75(6), G53–G64, doi:10.1190/1.3496476, 2010.

Doussan, C. and Ruy, S.: Prediction of unsaturated soil hydraulic conductivity with electrical conductivity, Water Resour. Res., 45(10), n/a–n/a, doi:10.1029/2008WR007309, 2009.

Duda, R. O., Hart, P. E. and Stork, D. G.: Pattern classification, 2nd ed., Wiley., 2001.

DWF: Greater water security with groundwater, København., 2013.

Ferré, T., Bentley, L., Binley, A., Linde, N., Kemna, A., Singha, K., Holliger, K., Huisman, J. A. and Minsley, B.: Critical Steps for the Continuing Advancement of Hydrogeophysics, Eos, Trans. Am. Geophys. Union, 90(23), 200, doi:10.1029/2009EO230004, 2009.

Gallardo, L. A. and Meju, M. A.: Characterization of heterogeneous near-surface materials by joint 2D inversion of dc resistivity and seismic data, Geophys. Res. Lett., 30(13), 1658, doi:10.1029/2003GL017370, 2003.

Glover, P. W. J.: 11.04 – Geophysical Properties of the Near Surface Earth: Electrical Properties, in Treatise on Geophysics, pp. 89–137, Elsevier., 2015.

Gómez-Hernández, J. J. and Srivastava, R.: ISIM3D - AN ANSI-C 3-DIMENSIONAL MULTIPLE INDICATOR CONDITIONAL SIMULATION PROGRAM, Comput. Geosci., 16(4), 395–440, 1990.

Goovaerts, P.: Geostatistics for Natural Resources Evaluation, Oxford University Press., 1997.

Hartigan, J. A.: Clustering algorithms, Wiley., 1975.

He, X., Højberg, A. L., Jørgensen, F. and Refsgaard, J. C.: Assessing hydrological model predictive uncertainty using stochastically generated geological models, Hydrol. Process., 29(19), 4293–4311, doi:10.1002/hyp.10488, 2015.

Henriksen, H. J., Troldborg, L., Nyegaard, P., Sonnenborg, T. O., Refsgaard, J. C. and Madsen, B.: Methodology for construction, calibration and validation of a national hydrological model for Denmark, J. Hydrol., 280(1-4), 52–71, doi:10.1016/S0022-1694(03)00186-0, 2003.

Herckenrath, D., Odlum, N. and Nenna, V.: Calibrating a Salt Water Intrusion Model with Time-Domain Electromagnetic Data, Groundwater, 51(3), 2013.

Hermans, T., Nguyen, F. and Caers, J.: Uncertainty in training image-based inversion of hydraulic head data constrained to ERT data: Workflow and case study, Water Resour. Res., 51(7), 5332–5352, doi:10.1002/2014WR016460, 2015.

Huysmans, M. and Dassargues, A.: Application of multiple-point geostatistics on modelling groundwater flow and transport in a cross-bedded aquifer (Belgium), Hydrogeol. J., 17(8), 1901–1911, doi:10.1007/s10040-009-0495-2, 2009.

Hyndman, D. W. and Gorelick, S. M.: Estimating lithologic and transport properties in three dimensions using seismic and tracer data: The Kesterson aquifer, Water Resour. Res., 32(9), 2659–2670, doi:10.1029/96wr01269, 1996.

Jain, A. K.: Data clustering: 50 years beyond K-means, Pattern Recognit. Lett., 31(8), 651–666, doi:10.1016/j.patrec.2009.09.011, 2010.

Jørgensen, F. and Sandersen, P. B. E.: Buried and open tunnel valleys in Denmark—erosion beneath multiple ice sheets, Quat. Sci. Rev., 25(11-12), 1339–1363, doi:10.1016/j.quascirev.2005.11.006, 2006.

Kahr, G. and Madsen, F. T.: Determination of the cation exchange capacity and the surface area of bentonite, illite and kaolinite by methylene blue adsorption, Appl. Clay Sci., 9(5), 327–336, doi:10.1016/0169-1317(94)00028-O, 1995.

Keating, E. H., Doherty, J., Vrugt, J. A. and Kang, Q.: Optimization and uncertainty assessment of strongly nonlinear groundwater models with high parameter dimensionality, Water Resour. Res., 46(10), n/a–n/a, doi:10.1029/2009WR008584, 2010.

Koch, J., He, X., Jensen, K. H. and Refsgaard, J. C.: Challenges in conditioning a stochastic geological model of a heterogeneous glacial aquifer to a comprehensive soft data set, Hydrol. Earth Syst. Sci., 18(8), 2907–2923, doi:10.5194/hess-18-2907-2014, 2014.

Lawrie, K. C., Carey, H., Christensen, N. B., Clarke, J., Lewis, S., Ivkovic, K. M. and S.K., M.: Evaluating the Role of Airborne Electromagnetics in Mapping Seawater Intrusion and Carbonate-Karstic Groundwater Systems in Australia, Canberra., 2012.

Linde, N., Finsterle, S. and Hubbard, S.: Inversion of tracer test data using tomographic

constraints, Water Resour. Res., 42(4), W04410, doi:10.1029/2004wr003806, 2006.

Linde, N., Renard, P., Mukerji, T. and Caers, J.: Geological Realism in Hydrogeological and Geophysical Inverse Modeling: a Review, Adv. Water Resour., 86, 86 – 101, doi:10.1016/j.advwatres.2015.09.019, 2015.

Lloyd, S.: Least squares quantization in PCM, IEEE Trans. Inf. Theory, 28(2), 129–137, doi:10.1109/TIT.1982.1056489, 1982.

Ma, C. and Eggleton, R.: Cation exchange capacity of kaolinite, Clays Clay Miner., 47(2), 174–180, 1999.

Margat, J. F. and van der Gun, J.: Groundwater around the world : a geographic synopsis, CRC Press, Boca Raton., 2013.

Meier, P., Kalscheuer, T., Podgorski, J. E., Kgotlhang, L., Green, A. G., Greenhalgh, S., Rabenstein, L., Doetsch, J., Kinzelbach, W., Auken, E., Mikkelsen, P., Foged, N., Jaba, B. C., Tshoso, G. and Ntibinyane, O.: Hydrogeophysical investigations in the western and north-central Okavango Delta (Botswana) based on helicopter and ground-based transient electromagnetic data and electrical resistance tomography, GEOPHYSICS, 79(5), B201–B211, doi:10.1190/geo2014-0001.1, 2014.

Meju, M. A. and Everett, M. E.: Near-surface controlled-source electromagnetic induction: Background and recent advances, in Hydrogeophysics, edited by Y. Rubin and S. S. Hubbard, p. 28, Springer Netherlands, Dordrecht., 2005.

Muffels, C., Wang, X., Matthew Tonkin, A. and Neville, C.: User's Guide for mod-PATH3DU A groundwater path and travel-time simulator, Bethesda, Maryland., 2014.

Møller, I., Jørgensen, F., Søndergaard, V., Ditlefsen, C. and Vest Christiansen, A.: Compilation of a Resistivity Atlas of Danish lithologies based on direct resistivity measurements and wireline logging data, ASEG Ext. Abstr. 2015 24th Int. Geophys. Conf. Exhib., 4, 2015.

Neuman, S. P. and Yakowitz, S.: A statistical approach to the inverse problem of aquifer hydrology: 1. Theory, Water Resour. Res., 15(4), 845–860, doi:10.1029/WR015i004p00845, 1979.

Oplandsråd: Oplandsråd for Norsminde Fjord, [online] Available from: http://oplandsråd-norsminde-fjord.dk/oplandet/ (Accessed 2 May 2016), 2013.

Panday, S., Langevin, C. D., Niswonger, R. G., Ibaraki, M. and Hughes, J. .: MODFLOW-USG version 1.3.00: An unstructured grid version of MODFLOW for simulating groundwater flow and tightly coupled processes using a control volume finite-difference formulation, in U.S. Geological Survey Techniques and Methods 6–A45, p. 78, Reston, Virginia., 2015.

Pebesma, E. J.: Multivariable geostatistics in S: the gstat package, Comput. Geosci., 30, 683–691, 2004.

Paasche, H., Tronicke, J., Holliger, K., Green, A. G. and Maurer, H.: Integration of diverse physical-property models: Subsurface zonation and petrophysical parameter estimation based on fuzzy c-means cluster analyses, Geophysics, 71(3), H33–H44, doi:10.1190/1.2192927, 2006.

Rasmussen, P., Sonnenborg, T. O., Goncear, G. and Hinsby, K.: Assessing impacts of climate change, sea level rise, and drainage canals on saltwater intrusion to coastal aquifer, Hydrol. Earth Syst. Sci., 17(1), 421–443, doi:10.5194/hess-17-421-2013, 2013.

Refsgaard, J. C., van der Sluijs, J. P., Brown, J. and van der Keur, P.: A framework for dealing with uncertainty due to model structure error, Adv. Water Resour., 29(11), 1586–1597, doi:10.1016/j.advwatres.2005.11.013, 2006.

Revil, A. and Cathles, L. M.: Permeability of shaly sands, Water Resour. Res., 35(3), 651–662, doi:10.1029/98WR02700, 1999.

Rhoades, J., Raats, P. and Prather, R.: EFFECTS OF LIQUID-PHASE ELECTRICAL-CONDUCTIVITY, WATER-CONTENT, AND SURFACE CONDUCTIVITY ON BULK SOIL ELECTRICAL-CONDUCTIVITY, SOIL Sci. Soc. Am. J., 40(5), 651–655, 1976.

Rhoades, J., Manteghi, N., Shouse, P. and Alves, W.: SOIL ELECTRICAL-CONDUCTIVITY AND SOIL-SALINITY - NEW FORMULATIONS AND CALIBRATIONS, SOIL Sci. Soc. Am. J., 53(2), 433–439, 1989.

Ronayne, M. J., Gorelick, S. M. and Caers, J.: Identifying discrete geologic structures that produce anomalous hydraulic response: An inverse modeling approach, Water Resour. Res., 44(8), n/a–n/a, doi:10.1029/2007WR006635, 2008.

Rubin, Y. and Hubbard, S. S., Eds.: Hydrogeophysics, Springer Netherlands, Dordrecht., 2005.

Sandersen, P. B. E. and Jorgensen, F.: Buried Quaternary valleys in western Denmark - occurrence and inferred implications for groundwater resources and vulnerability, J. Appl. Geophys., 53(4), 229–248, doi:10.1016/j.jappgeo.2003.08.006, 2003.

Seifert, D., Sonnenborg, T. O., Refsgaard, J. C., Hojberg, A. L. and Troldborg, L.: Assessment of hydrological model predictive ability given multiple conceptual geological models, Water Resour. Res., 48, W06503, doi:10.1029/2011wr011149, 2012.

Steinmetz, D., Winsemann, J., Brandes, C., Siemon, B., Ullmann, A., Wiederhold, H. and Meyer, U.: Towards an improved geological interpretation of airborne electromagnetic data: a case study from the Cuxhaven tunnel valley and its Neogene host sediments (northwest Germany), Netherlands J. Geosci., 94(02), 201–227, doi:10.1017/njg.2014.39, 2014.

Sulzbacher, H., Wiederhold, H., Siemon, B., Grinat, M., Igel, J., Burschil, T., Günther, T. and Hinsby, K.: Numerical modelling of climate change impacts on freshwater lenses on the North Sea Island of Borkum using hydrological and geophysical methods, Hydrol. Earth Syst. Sci., 16(10), 3621–3643, doi:10.5194/hess-16-3621-2012, 2012.

Sørensen, K. I. and Auken, E.: SkyTEM - a new high-resolution helicopter transient electromagnetic system, Explor. Geophys., 35(3), 194–202, 2004.

Viezzoli, A., Auken, E. and Munday, T.: Spatially constrained inversion for quasi 3D modelling of airborne electromagnetic data – an application for environmental assessment in the Lower Murray Region of South Australia, Explor. Geophys., 40(2), 173, doi:10.1071/EG08027, 2009.

Vrugt, J. A., Diks, C. G. H., Gupta, H. V., Bouten, W. and Verstraten, J. M.: Improved treatment of uncertainty in hydrologic modeling: Combining the strengths of global optimization and data assimilation, Water Resour. Res., 41(1), n/a–n/a, doi:10.1029/2004WR003059, 2005.

Waxman, M. and Smits, L.: ELECTRICAL CONDUCTIVITIES IN OIL-BEARING SHALY SANDS, Soc. Pet. Eng. J., 8(2), 107–&, 1968.

Western, A. W., Blöschl, G. and Grayson, R. B.: Toward capturing hydrologically

significant connectivity in spatial patterns, Water Resour. Res., 37(1), 83–97, doi:10.1029/2000WR900241, 2001.

Zhou, H. Y., Gomez-Hernandez, J. J. and Li, L. P.: Inverse methods in hydrogeology: Evolution and recent trends, Adv. Water Resour., 63, 22–37, doi:10.1016/j.advwatres.2013.10.014, 2014.

12 Papers

I Foged, N., Marker, P. A., Christansen, A. V., Bauer-Gottwein, P., Jørgensen, F., Høyer, A.-S., and Auken, E.: Large-scale 3-D modeling by integration of resistivity models and borehole data through inversion, Hydrol. Earth Syst. Sci., 18, 4349-4362, doi:10.5194/hess-18-4349-2014, 2014.

II Marker, P. A., Ferré, T., Vilhelmsen, T. N., Tuller, M., Bauer-Gottwein, P.: Can groundwater model hydrostratigraphy be determined from electrical conductivity and clay fraction? *Manuscript*.

III Marker, P. A., Foged, N., He, X., Christiansen, A. V., Refsgaard, J. C., Auken, E., and Bauer-Gottwein, P.: Performance evaluation of groundwater model hydrostratigraphy from airborne electromagnetic data and lithological borehole logs, Hydrol. Earth Syst. Sci., 19, 3875-3890, doi:10.5194/hess-19-3875-2015, 2015.

IV Marker, P. A., Villumsen, T. N., Foged, N., Wernberg, T., Auken, E., and Bauer-Gottwein, P.: Probabilistic predictions from groundwater model informed with airborne EM data. *Submitted 28 April 2016.*

TEXT FOR WWW-VERSION (without papers)

In this online version of the thesis, Paper **I-IV** are not included but can be obtained from electronic article databases, e.g. via www.orbit.dtu.dk or on request from DTU Environment, Technical University of Denmark, Bygningstorvet, Building 115, 2800 Kgs. Lyngby, Denmark, info@env.dtu.dk.